PREDICTION OF THRUST FORCE IN TWIST DRILL

A thesis submitted in partial fulfillment of
the requirement for the award of

MASTER OF ENGINEERING
IN
CAD/CAM & ROBOTICS

Submitted By

CHITRARTH KISHORE
Roll No. 800981007

Under the Guidance of

Mr. JASWINDER SINGH SAINI
Assistant Professor
Deptt. of Mech. Engg.
TU, Patiala

DEPARTMENT OF MECHANICAL ENGINEERING
THAPAR UNIVERSITY
PATIALA-147004, INDIA
(2011)

CERTIFICATE

I hereby declare that the work which is being presented in this thesis entitled, **"PREDICTION OF THRUST FORCE IN TWIST DRILL"** in partial fulfillment of the award of the **MASTER OF ENGINEERING IN CAD/CAM & ROBOTICS** submitted in the **MECHANICAL ENGINEERING DEPARTMENT , THAPAR UNIVERSITY, PATIALA,** is an authentic record of the initial work carried out by me under the guidance of **Mr. JASWINDER SINGH SAINI, Assistant Professor, Mechanical Engineering Department , Thapar University, Patiala** and refers other researcher's work which is duly listed in the reference section.

The matter embodied in this thesis has not been submitted in partial or full to any other university or institute for the award of any degree.

Kishore

(CHITRARTH KISHORE)

Dated: 4-7-2011

This is to certify that above declaration made by the student concerned is correct to the best of my knowledge and belief

4/7/2011

(Mr. JASWINDER SINGH SAINI)
Assistant Professor,MED
Thapar University, Patiala

Countersigned by

(Dr. AJAY BATISH)
Professor & Head,MED
Thapar University, Patiala

(Dr. S. K. MOHAPATRA)
Dean, Academic Affairs
Thapar University, Patiala

i

ACKNOWLEDGEMENT

I would like to express a deep sense of gratitude and thank profusely to my guide **Mr. JASWINDER SINGH SAINI** for his sincere & invaluable guidance, suggestions and attitude, which inspired me to Submit Seminar Report in the present form. His dynamism and diligent enthusiasm have been highly instrumental in keeping my spirits high. His flawless and forthright suggestions blended with an innate intelligent application have crowned my task with success.

I am also thankful to **Dr. AJAY BATISH,** Professor & Head, Department of Mechanical Engineering for his encouragement and inspiration for execution of the seminar work.

I am deeply indebted to my parents for their inspiration and ever encouraging moral support, which enabled me to pursue my studies.

I am also very thankful to the entire faculty and staff members of Mechanical Engineering Department for their intellectual support and cooperation.

Kishore

CHITRARTH KISHORE

Roll No. 800981007

ABSTRACT

The present study is focused on predicting the thrust force in drilling with twist drill using finite element technique. The twist drill is versatile and can be used on a variety of materials. The approach is based on representing the cutting forces along the cutting lips as a series of oblique sections. For each section a Eulerian finite element method is used to simulate the cutting forces. The section forces were combined to predict the overall forces.

A program in C language is developed using the above said approach. Thereafter it's validation is done by experimental results given by Strenkowski *et al.* [13] where the same approach is being used. The values are calculated for machining of AISI 1020 steel.

INDEX

LIST OF FIGURES

LIST OF TABLES

CHAPTER 1 INTRODUCTION

The progress and the prosperity of human civilization are governed and judged mainly by improvement and maintenance of standard of living through availability or production of ample and quality goods and services for Men's Material Welfare (MMW) in all respects covering housing, clothing, medicine, education, transport, communication and also entertainment. The successful creation of (MMW) depends mainly on

- Availability of Natural Resources (NR).
- Exertion of Human Effort (HE); both physical and mental.
- Development and use of power tools and machines (Tools).

This can be depicted in a simple form,

$$MMR = NR(HE)^{TOOLS}$$

Where,

NR: refers to air, water, heat and light, plants and animals and solid and liquid minerals.

TOOLS: refers to power plants, chemical plants, steel plants and machine tools etc. which magnify human capability.

This clearly indicates the important roles of the components; NR, HE and TOOLS on achieving MMW and progress of civilization.

Production or manufacturing can be simply defined as value addition processes by which raw materials of low utility and value due to its inadequate material properties and poor or irregular size, shape and finish are converted into high utility and valued products with definite dimensions, forms and finish imparting some functional ability. A typical example of manufacturing is schematically shown in Fig. 1.1.

A lump of mild steel of irregular shape, dimensions and surface, which had almost no use and value, has been converted into a useful and valuable product like bolt by a manufacturing process which imparted suitable features, dimensional accuracy and surface finish, required for fulfilling some functional requirements.

1.1 BROAD CLASSIFICATION OF ENGINEERING MANUFACTURING PROCESSES

It is extremely difficult to tell the exact number of various manufacturing processes existing and is being practiced presently because a spectacularly large number of processes have been developed till now and the number is still increasing exponentially with the growing demands and rapid progress in science and technology. However, all such manufacturing processes can be broadly classified in four major groups as follows:

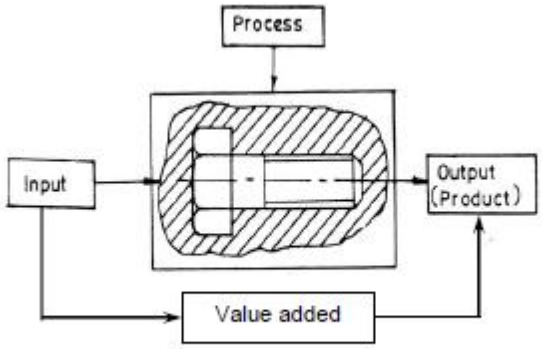

Fig. 1.1 Value additions by manufacturing.

(a) Shaping or **forming**

Manufacturing a solid product of definite size and shape from a given material taken in three possible states:

• In solid state – e.g. forging rolling, extrusion, drawing etc.

• In liquid or semi-liquid state – e.g. casting, injection moulding etc.

• In powder form – e.g. powder metallurgical process.

(b) Joining process

Welding, brazing, soldering etc.

(c) Removal process

Machining (Traditional or Non-traditional), Grinding etc.

(d) Regenerative manufacturing

Production of solid products in layer by layer from raw materials in different form:

- Liquid – e.g. Stereolithography.
- Powder – e.g. Selective Sintering.

- Sheet – e.g. LOM (Laminated Object Manufacturing).
- Wire – e.g. FDM (Fused Deposition Modelling).

Out of the aforesaid groups, Regenerative Manufacturing is the latest one which is generally accomplished very rapidly and quite accurately using CAD and CAM for Rapid Prototyping and Tooling.

1.2 MACHINING – PURPOSE, PRINCIPLE AND DEFINITION

1.2.1 Purpose of Machining

Most of the engineering components such as gears, bearings, clutches, tools, screws and nuts etc. need dimensional and form accuracy and good surface finish for serving their purposes. Preforming like casting, forging etc. generally cannot provide the desired accuracy and finish. For that such preformed parts, called blanks, need semi-finishing and finishing and it is done by machining and grinding. Grinding is also basically a machining process.

Machining to high accuracy and finish essentially enables a product to:

- Fulfill its functional requirements.
- Improve its performance.
- Prolong its service.

1.2.2 Principle of Machining

The basic principle of machining is typically illustrated in Fig. 1.2.

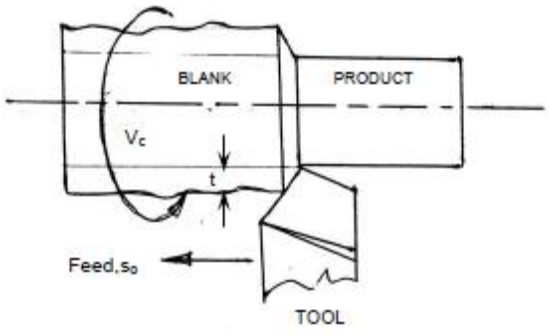

Fig. 1.2 Principal of machining (turning).

A metal rod of irregular shape, size and surface is converted into a finished rod of desired dimension and surface by machining by proper relative motions of the tool-work pair.

1.2.3 Definition of Machining

Machining is an essential process of finishing by which jobs are produced to the desired dimensions and surface finish by gradually removing the excess material from the preformed blank in the form of chips with the help of cutting tool(s) moved past the work surface(s).

1.3 MACHINING REQUIREMENTS

The essential basic requirements for machining work are schematically illustrated in Fig. 1.3.

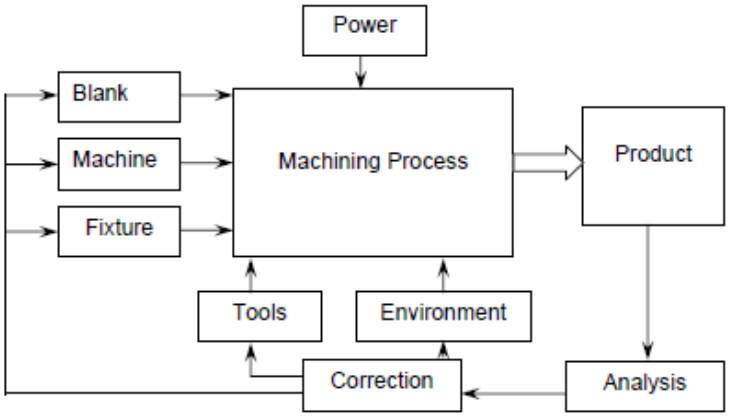

Fig. 1.3 Requirements for machining.

The blank and the cutting tool are properly mounted (in fixtures) and moved in a powerful device called machine tool enabling gradual removal of layer of material from the work surface resulting in its desired dimensions and surface finish. Additionally some environment called cutting fluid is generally used to ease machining by cooling and lubrication.

1.4 CUTTING TOOLS

Both material and geometry of the cutting tools play very important roles on their performances in achieving effectiveness, efficiency and overall economy of machining.

Cutting tools may be classified according to the number of major cutting edges (points) involved as follows:

- Single point: e.g. turning tools, shaping, planning and slotting tools and boring tools.
- Double (two) point: e.g. drills.
- Multipoint (more than two): e.g. milling cutters, broaching tools, hobs, gear shaping cutters etc.

1.5 GEOMETRY OF SINGLE POINT TURNING TOOLS

1.5.1 Concept of Rake and Clearance Angles of Cutting Tools

The word tool geometry is basically referred to some specific angles or slope of the salient faces and edges of the tools at their cutting point. Rake angle and clearance angle are the most significant for all the cutting tools.

The concept of rake angle and clearance angle will be clear from some simple operations shown in Fig. 1.4.

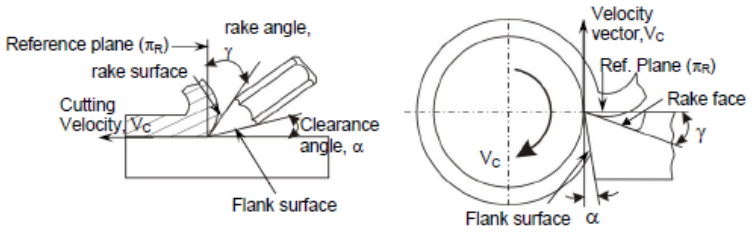

Fig. 1.4 Rake and clearance angles of cutting tools.

Definition:

- Rake angle (γ): Angle of inclination of rake surface from reference plane.
- Clearance angle (α): Angle of inclination of clearance or flank surface from the finished surface.

Rake angle is provided for ease of chip flow and overall machining. Rake angle may be positive, or negative or even zero as shown in Fig. 1.5.

Relative advantages of such rake angles are:

- Positive rake – helps reduce cutting force and thus cutting power requirement.
- Negative rake – to increase edge-strength and life of the tool.

- Zero rake – to simplify design and manufacture of the form tools.

Clearance angle is essentially provided to avoid rubbing of the tool (flank) with the machined surface which causes loss of energy and damages of both the tool and the job surface. Hence, clearance angle is a must and must be positive ($3^0 - 15^0$ depending upon tool-work materials and type of the machining operations like turning, drilling, boring etc.)

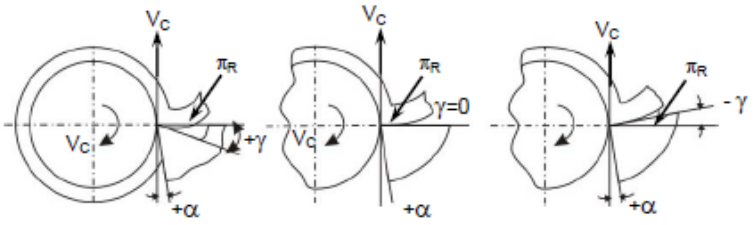

a) Positive rake (b) Zero rake (c) Negative rake

Fig. 1.5 Three possible types of rake angles.

1.5.2 Systems of Description of Tool Geometry

- Tool-in-Hand System – where only the salient features of the cutting tool point are identified or visualized as shown in Fig. 1.6. There is no quantitative information, *i.e.*, value of the angles.
    - Machine Reference System – ASA system.
    - Tool Reference Systems.
        - Orthogonal Rake System (ORS).
        - Normal Rake System (NRS).
    - Work Reference System (WRS).

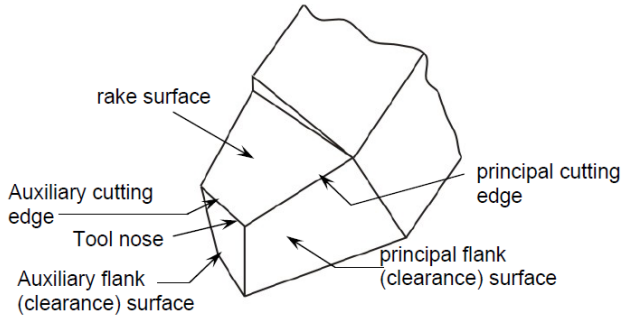

Fig. 1.6 Basic features of single point tool (turning) in Tool-in-hand system.

1.6 MECHANISM OF CHIP FORMATION IN MACHINING

Machining is a semi-finishing or finishing process essentially done to impart required or stipulated dimensional and form accuracy and surface finish to enable the product to:

- Fulfill its basic functional requirements.
- Provide better or improved performance.
- Render long service life.

Machining is a process of gradual removal of excess material from the preformed blanks in the form of chips. The form of the chips is an important index of machining because it directly or indirectly indicates:

- Nature and behavior of the work material under machining condition.
- Specific energy requirement (amount of energy required to remove unit volume of work material) in machining work.
- Nature and degree of interaction at the chip-tool interfaces.

The form of machined chips depends mainly upon:

- Work material.
- Material and geometry of the cutting tool.
- Levels of cutting velocity and feed and also to some extent on depth of cut.
- Machining environment or cutting fluid that affects temperature and friction at the chip- tool and work-tool interfaces.

Knowledge of basic mechanism(s) of chip formation helps to understand the characteristics of chips and to attain favorable chip forms.

1.6.1 Mechanism of Chip Formation in Machining Ductile Materials

During continuous machining the uncut layer of the work material just ahead of the cutting tool (edge) is subjected to almost all sided compression as indicated in Fig. 1.7. The force exerted by the tool on the chip arises out of the normal force (N) and frictional force (F) as indicated in Fig. 1.7. Due to such compression, shear stress develops, within that compressed region, in different magnitude, in different directions and rapidly increases in magnitude. Whenever and wherever the value of the shear stress reaches or exceeds the shear strength of that work material in the deformation region, yielding or

slip takes place resulting shear deformation in that region and the plane of maximum shear stress.

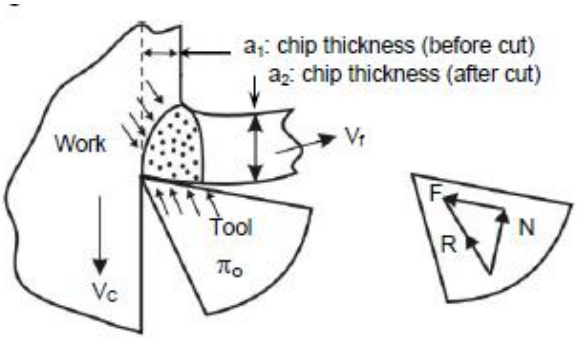

Fig. 1.7 Compression of work material (layer) ahead of the tool tip.

But the forces causing the shear stresses in the region of the chip quickly diminishes and finally disappears while that region moves along the tool rake surface towards and then goes beyond the point of chip-tool engagement. As a result the slip or shear stops propagating long before total separation takes place. In the mean time the succeeding portion of the chip starts undergoing compression followed by yielding and shear. This phenomenon repeats rapidly resulting in formation and removal of chips in thin layer by layer. This phenomenon has been explained in a simple way by Piispannen [22] using a card analogy as shown in Fig. 1.8.

In actual machining chips also, such serrations are visible at their upper surface as indicated in Fig. 1.8. The lower surface becomes smooth due to further plastic deformation due to intensive rubbing with the tool at high pressure and temperature. The pattern of shear deformation by lamellar sliding, indicated in the model, can also be seen in actual chips by proper mounting, etching and polishing the side surface of the machining chip and observing under microscope. The pattern and extent of total deformation of the chips due to the primary and the secondary shear deformations of the chips ahead and along the tool face as indicated in Fig. 1.9 depend upon:

- Work material.
- Tool; material and geometry.
- The machining speed (V_C) and feed (s_O).
- Cutting fluid application.

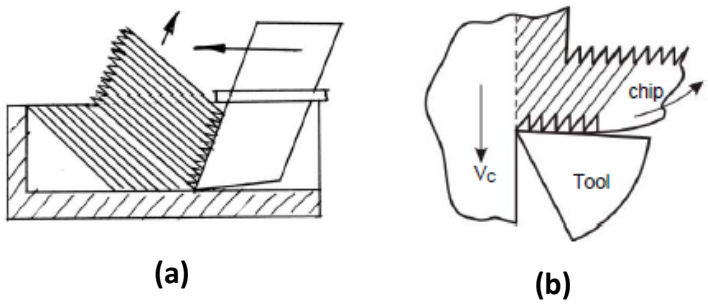

(a) Shifting of the postcards by partial

(b) Chip formation by shear in sliding against each other lamella

Fig. 1.8 Piispanen model of card analogy to explain chip formation in machining ductile materials.

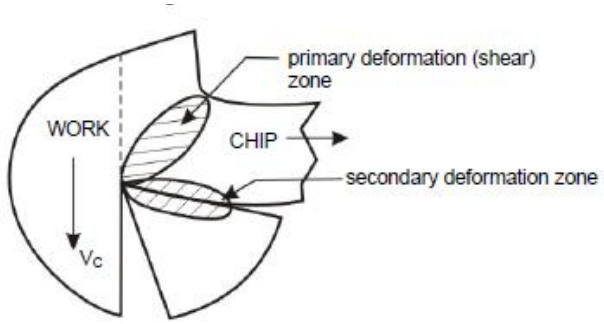

Fig. 1.9 Primary and secondary deformation zones in the chip.

The overall deformation process causing chip formation is quite complex and hence needs thorough experimental studies for clear understanding the phenomena and its dependence on the affecting parameters. The feasible and popular experimental methods for this purpose are:

- Study of deformation of rectangular or circular grids marked on the side surface as shown in Fig. 1.10.
- Microscopic study of chips frozen by drop tool or quick stop apparatus.
- Study of running chips by high speed camera fitted with low magnification microscope.

It has been established by several analytical and experimental methods including circular grid deformation that though the chips are initially compressed ahead of the tool tip, the final deformation is accomplished mostly by shear in machining ductile materials.

However, machining of ductile materials generally produces flat, curved or coiled continuous chips.

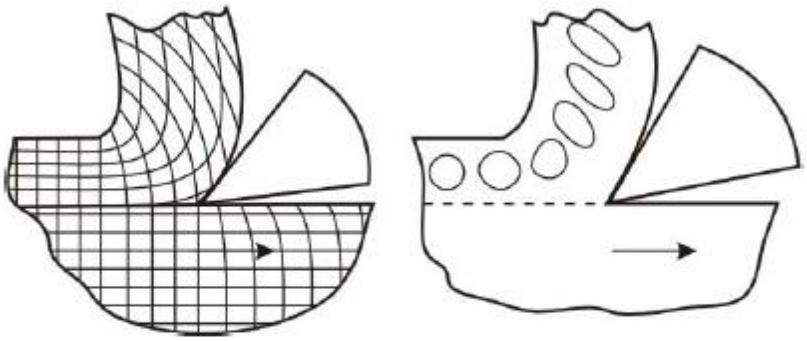

(a) rectangular grids, (b) circular grids

Fig. 1.10 Pattern of grid deformation during chip formation.

1.6.2 Mechanism of Chip Formation in Machining Brittle Materials

The basic two mechanisms involved in chip formation are :

- Yielding – generally for ductile materials.
- Brittle fracture – generally for brittle materials.

During machining, first a small crack develops at the tool tip as shown in Fig. 1.11 due to wedging action of the cutting edge. At the sharp crack-tip stress concentration takes place. In case of ductile materials immediately yielding takes place at the crack-tip and reduces the effect of stress concentration and prevents its propagation as crack. But in case of brittle materials the initiated crack quickly propagates, under stressing action, and total separation takes place from the parent workpiece through the minimum resistance path as indicated in Fig. 1.11.

Machining of brittle material produces discontinuous chips and mostly of irregular size and shape. The process of forming such chips is schematically shown in Fig. 1.12.

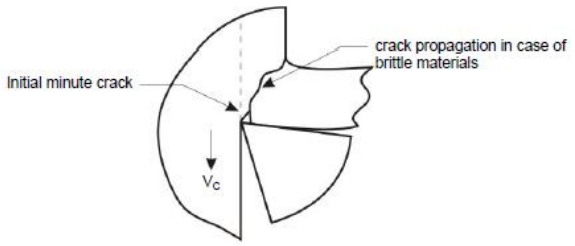

Fig. 1.11 Development and propagation of crack causing chip separation.

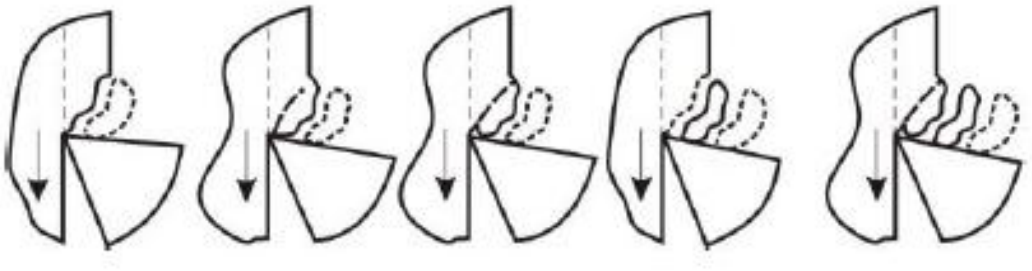

(a) **(b)** **(c)** **(d)** **(e)**

(a) separation,(b) swelling,(c) further swelling,(d) separation,(e) swelling again

Fig. 1.12 Schematic view of chip formation in machining brittle materials.

1.7 DRILL

A drill or drill motor is a tool fitted with a cutting tool attachment or driving tool attachment, usually a drill bit or driver bit, used for drilling holes in various materials or fastening various materials together with the use of fasteners. The attachment is gripped by a chuck at one end of the drill and rotated while pressed against the target material. The tip, and sometimes edges, of the cutting tool does the work of cutting into the target material. This may be slicing off thin shavings (twist drills or auger bits), grinding off small particles (oil drilling), crushing and removing pieces of the workpiece (SDS masonry drill), countersinking, counterboring, or other operations. Drills are commonly used in woodworking, metalworking, construction and do-it-yourself projects. Specially designed drills are also used in medicine, space missions and other applications.

1.7.1 History of Drills

A wooden drill handle and other carpentry tools found on board the 16th century carrack Mary Rose. The earliest drills were bow drills which date back to the ancient Harappans

and Egyptians. The drill press as a machine tool evolved from the bow drill and is many centuries old. It was powered by various power sources over the centuries, such as human effort, water wheels, and windmills, often with the use of belts. With the coming of the electric motor in the late 19th century, there was a great rush to power machine tools with such motors, and drills were among them. The invention of the first electric drill is credited to Arthur James Arnot and William Blanch Brain in 1889, at Melbourne, Australia. Wilhelm Fein invented the portable electric drill in 1895, at Stuttgart, Germany. In 1917, Black & Decker patented a trigger-like switch mounted on a pistol-grip handle.

1.7.2 Types of Drills

There are many types of drills: some are powered manually, others use electricity (electric drill) or compressed air (pneumatic drill) as the motive power, and a minority is driven by an internal combustion engine (for example, earth drilling augers). Drills with a percussive action (hammer drills) are mostly used in hard materials such as masonry (brick, concrete and stone) or rock. Drilling rigs are used to bore holes in the earth to obtain water or oil. Oil wells, water wells, or holes for geothermal heating are created with large drilling rigs. Some types of hand-held drills are also used to drive screws and other fasteners. Some small appliances that have no motor of their own may be drill-powered, such as small pumps, grinders, etc.

1.7.3 General Classifications

A. Classification Based on Construction

- Solid Drills: Those made of one piece of material such as high speed steel.
- Tipped Solid Drills: Those having a body of one material with cutting lips made of another material brazed or otherwise bonded in place.
- Composite Drills: Those having cutting portions mechanically held in place.

B. Classification Based on Methods of Holding or Driving

- Straight Shank Drills: Those having cylindrical shanks which may be the same or different diameter than the body of the drill; the shanks may be made with or without driving flats, tang, grooves or threads.

- Taper Shank Drills: Those having conical shanks suitable for direct fitting into tapered holes in machine spindles, driving sleeves or sockets; tapered shanks generally have a driving tang.
- Taper Shank Square Drills: Those having tapered shanks with four flat sides for fitting a rachet or brace.
- Shell Core Drills: Core drills mountable on arbors specifically designed for the purpose; commonly used with shell reamer arbors.
- Threaded Shank Drills: Those made with threaded shanks generally used in close center multiple spindle applications or portable angle drilling tools.
- Beaded Shank Bits: Drills with flat shanks having raised beads parallel to the axis.

C. Classification Based on Number of Flutes

- Two-Flute Drills: The conventional type of twist drill used for originating holes.
- Single-Flute Drills: Those having only one flute, so only used for originating holes.
- Three-Flute Drills (Core Drills): Drills commonly used for enlarging and finishing, drilled, cast, or punched holes; they will not produce original holes.
- Four-Flute Drills (Core Drills): Used interchangeably with three-flute drills; they are of similar construction except for the number of flutes.

D. Classification Based on Hand of Cut

- Right-Hand Cut: When viewed from the cutting point the counterclockwise rotation of a drill in order to cut; the great majority of drills are made "right hand".
- Left-Hand Cut: When viewed from the cutting point the clockwise rotation of a drill in order to cut.

1.7.4 Nomenclature of Twist Drills and Other Terms Relating to Drilling

The following terms are used in the nomenclature of twist drill. These terms relate to the various geometry features and other terminologies used while carrying out a drilling process. Fig. 1.13, Fig. 1.14, Fig. 1.15 depicts the various geometry features described below.

- Axis: The imaginary straight line which forms the longitudinal center line of the drill.
- Back Taper: A slight decrease in diameter from front to back in the body of the drill.
- Body: The portion of the drill extending from the shank or neck to the outer corners of

the cutting lips.

- Body Diameter Clearance: That portion of the land that has been cut away so it will not rub against the walls of the hole.
- Built-Up Edge: An adhering deposit of nascent material on the cutting lip or the point of the drill.
- Chip Breaker: Nicks or Grooves designed to reduce the size of chips; they may be steps or grooves in the cutting lip or in the leading face of the land at or adjacent to the cutting lips.
- Chip Packing: The failure of chips to pass through the flute during cutting action.
- Chipping: The breakdown of a cutting lip or margin by loss of fragments broken away during the cutting action.
- Chisel Edge: The edge at the end of the web that connects the cutting lips.
- Chisel Edge Angle: The angle included between the chisel edge and the cutting lip, as viewed from the end of the drill.
- Clearance: The space provided to eliminate undesirable contact between the drill and the workpiece.
- Drill Diameter: The diameter over the margins of the drill measured at the point.
- Flat Drill: A drill whose flutes are produced by two parallel or tapered flats.
- Flat (Spade) Drill: A removable cutting drill tip usually attached to a special holder designed for this purpose; generally used for drilling or enlarging cored holes.
- Flutes: Helical or straight grooves cut or formed in the body of the drill to provide cutting lips, to permit removal of chips, and to allow cutting fluid to reach the cutting lips.
- Flute Length: The length from the outer corners of the cutting lips to the extreme back end of the flutes; it includes the sweep of the tool used to generate the flutes and, therefore, does not indicate the usable length of the flutes.
- Helix Angle: The angle made by the leading edge of the land with a plane containing the axis of the drill.
- Land: The peripheral portion of the body between adjacent flutes.
- Land Width: The distance between the leading edge and the heel of the land measured

at a right angle to the leading edge.

- Lead: The axial advance of a leading edge of the land in one turn around the circumference.
- Neck: The section of reduced diameter between the body and the shank of a drill Oil.
- Grooves: Longitudinal straight or helical grooves in the shank, or grooves in the lands of a drill to carry cutting fluid to the cutting lips.
- Oil Holes or Tubes: Holes through the lands or web of a drill for passage of cutting fluid to the cutting lips.
- Overall Length: The length from the extreme end of the shank to the outer corners of the cutting lips; it does not include the conical shank end often used on straight shank drills, nor does it include the conical cutting point used on both straight and taper shank drills.
- Point: The cutting end of a drill, made up of the ends of the lands and the web; in form it resembles a cone, but departs from a true cone to furnish clearance behind the cutting lips.
- Point Angle: The angle included between the cutting lips projected upon a plane parallel to the drill axis and parallel to the two cutting lips.
- Relief: The result of the removal of tool material behind or adjacent to the cutting lip and leading edge of the land to provide clearance and prevent rubbing (heel drag).
- Shank: The part of the drill by which it is held and driven.
- Step Drill: A multiple diameter drill with one set of drill lands which are ground to different diameters.
- Straight Flutes: Flutes which form lands lying in an axial plane.
- Tang: The flattened end of a taper shank, intended to fit into a driving slot in a socket.
- Taper Drill: A drill with part or all of its cutting flute length ground with a specific taper to produce tapered holes; they are used for drilling the original hole or enlarging an existing hole.
- Web: The central portion of the body that joins the lands; the extreme end of the web forms the chisel edge on a two-flute drill.
- Web Thickness: The thickness of the web at the point, unless another specific location is indicated.

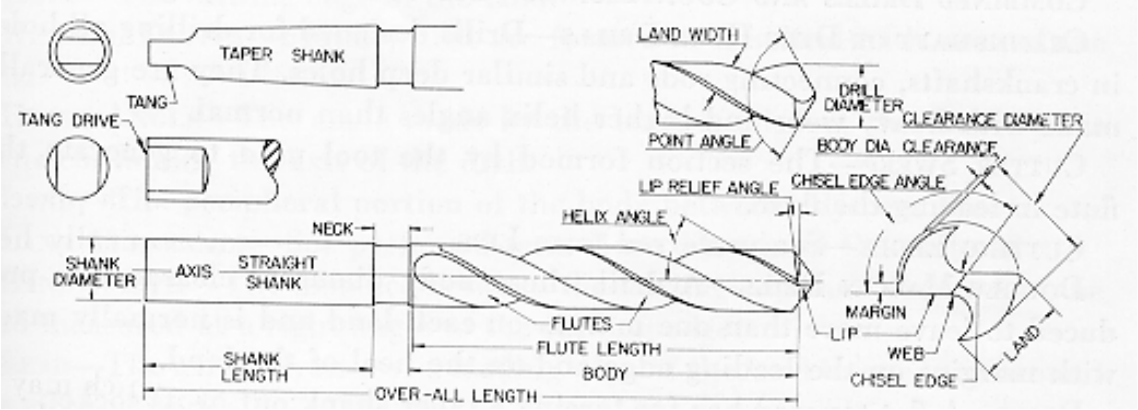

Fig. 1.13 Illustrations of terms applying to twist drill.

Fig. 1.14 Types of twist drill.

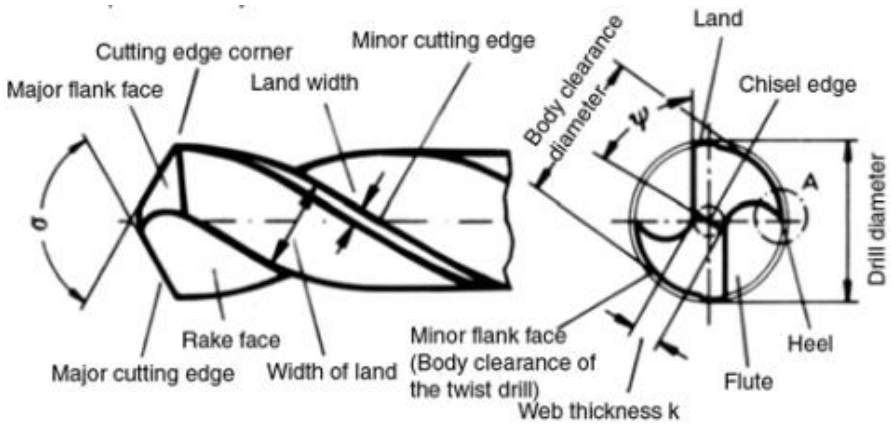

Fig. 1.15 Twist Drill Geometry (σ = point angle, ψ = chisel edge angle).

1.7.5 Forces Acting on Drill

The various forces acting on a drill are shown in Fig. 1.16. All the elements of a drill are subject to certain forces in drilling. Resolving the resultant forces of resultant forces of resistance to cutting at each point of the lip we obtain three forces (F_Z , F_V and F_H)

acting in directions mutually perpendicular to each other. The Horizontal force (F_H) acting on both lips are considered to counter balance each other. The Vertical force (F_V) also called as thrust force comprises of the forces F_{V_1} , F_{V_2} and F_C . The forces F_C and F_m are not shown. The force F_{V_1} acts on the web. This force is quite large and is about 60% of the total thrust force. This force F_{V_2} acts on each of the two lips and forms the real cutting force which depends upon the work material, cutting variables and cutting point geometry and is about 37% of the total thrust force. The forces F_C and F_m are of smaller magnitude. The force F_C is due to the rubbing of chips, flow from the hole against the sides of the hole and flutes on the drill. This force this force is about 1% of the total thrust force. The force F_M is due to the rubbing action of margin of the drill against the sides of the hole and is about 2% of thrust force.

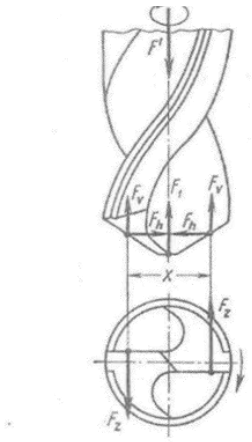

Fig. 1.16 Forces acting on drill.

In order that the drill to penetrate into the work piece the thrust force (*F*) applied to it by the machine must overcome the sum of resistances acting along the drill axis.

$$F > \sum F_{V_1} + 2F_{V_2} + F_C + F_m$$

The force F_Z sets up the moment of resistance (M_r)

$$M_r = F_Z.S$$

The total moment of the forces of resistance (*M*) to cutting is made up of the following moments.

1. Moment of forces F_Z i.e. (M_r).

2. Moment of forces due to scraping and friction on the chisel edge (M_C).
3. Moment of the friction forces on the margins (M_m).
4. Moment of the forces of friction of the chip on the drill and on the machined surface (M_d).

$$M = M_r + M_c + M_m + M_d$$

The total moment of resistance should be overcome by the available torque of the drilling machine.

1.7.6 Power of Drilling

When a drill is cutting it has to overcome the resistance offered by the metal and a twisting effort is necessary to turn it. The effort is called turning moment or torque on the drill. The torque required to operate a drill depends upon various factors. The relationship between torque, diameter of drill and feed is as follows:

$$T_1 = C.f^{0.75}.D^{1.8}$$

Where

T_1 = Torque in *Nm*

f= Drill feed in *mm/rev*

D= Diameter of drill in *mm*

C= Constant depending upon the material being drilled.

1.7.7 Effect of Various Factors in the Axial Thrust and Torque in Drilling

Drilling torque and axial thrust are functions mainly on the following factors:

- **Work piece material:** The higher tensile strength or hardness of the material, the greater the axial thrust and the moment of the forces of resistance to cutting in drilling. This relationship can be expressed mathematically by the following equation: In drilling steel with high-speed steel drills:

$$F = C_1\sigma_t^{0.75}$$

$$M = C_2\sigma_t^{0.75}$$

In drilling grey cast iron with carbide-tipped drills:

$$F = C_3 Bhn^{1.08}$$

$$M = C_4 Bhn^{0.5}$$

- **Drill diameter and feed:** The larger the drill diameter and the rate of feed per revolution, the larger the cross sectional area of the undeformed chip will be, the greater the resistance of the chip formation and, consequently, the greater the axial thrust and torque.

  Experimental research has indicated that the drill diameter has a greater effect in increasing *F* and *M* than the rate of feed. The reason is that the drill diameter seems to represent the depth of cut in drilling and, as such, has more influence on the forces acting in cutting than the feed.

- **Drill geometry:** The helix angle (*W*) of the flutes affects *F* and *M* in as much as it determines the rake angle of the drill. It follows from the formulae that the larger helix is the larger rake angle will be at each point of the lip, the more easily the chip is formed.

$$\tan\gamma_x = \frac{r_x \tan w}{R\sin\varphi}$$

  Consequently, lower the axial thrust force (*F*) and the moment of forces of resistance (*M*) as shown in Fig. 1.17, this reduction is more marked up to a value of 30^0.

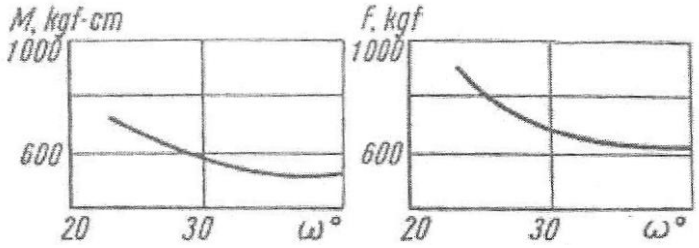

(a) **(b)**

Fig. 1.17 Effect of flute helix angle (a) on the torque, (b) on the axial thrust.

The point angle (2φ) affect the ratio of forces horizontal and vertical, as well as the undeformed chip thickness. Therefore, it cannot but affect thrust (*F*) and torque (*M*) upon reduction in the point angle, the horizontal forces increase and the vertical force decrease in the same manner as both forces are changed upon a reduction of the plan approach angle of a single point tool in turning, as shown in Fig. 1.18.

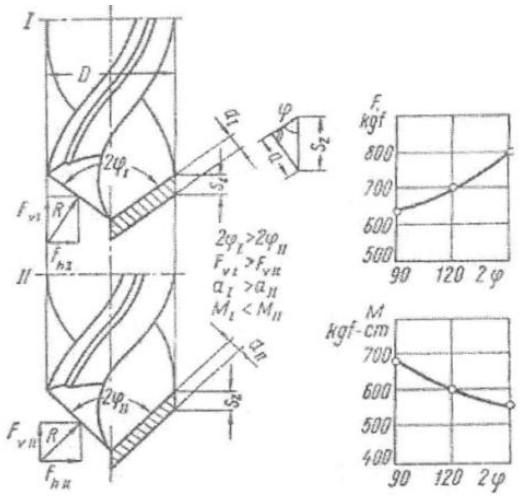

Fig. 1.18 Effect of the point angle on the axial thrust and torque.

A reduction in vertical forces, in turn, leads to reduction in the axial thrust force (*F*) likewise, an increase in point angle leads to an increase in axial thrust force (*F*).

- **Cutting fluid efficiency:** The favorable action of cutting fluids is manifested in drilling as well since the cutting process in drilling is accompanied by the same phenomenon as in turning. Consequently, the use of suitable cutting fluids and especially surface active emulsions, leads to a reduction in axial thrust (feeding force) and the torque, in comparison with drilling dry, by 10-30% for steel, 10-18% for cast iron and 30-40% for aluminum alloys.
- **Drilling depth:** The cutting condition deteriorates with an increase in depth of the hole being drilled. Difficulties are encountered with cutting fluid delivery and chip ejection; heat evolution is increased, as in the degree of work hardening. All of these factors reduce the drill life and increase the axial thrust and torque. Cutting at a great depth can be facilitated by grinding chip breaker grooves on the drill which divide the chip, making it easier to eject, and reduce the heat generation, axial thrust and torque.
- **Drill wear:** With the increase in flank wear of the drill (on the lip relief surface), as shown in Fig. 1.19, *F* and *M* are increased. In comparison with a sharp drill, the use of dull drill raises *F* and *M* by 10-16%.

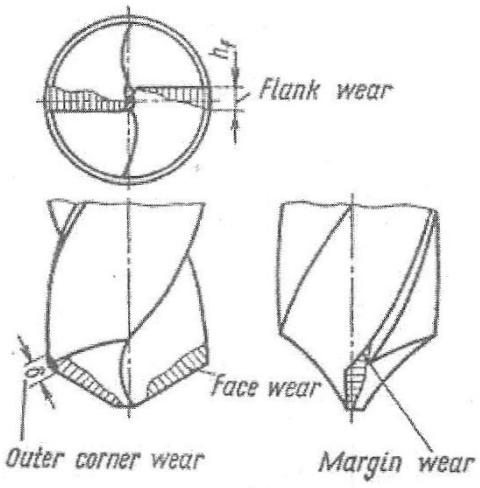

Fig. 1.19 Wear of high-speed steel twist drill.

- **Cutting speed:** Axial thrust (*F*) and torque (*M*) are first increased and then decreased with an increase in the cutting speed.

CHAPTER 2 LITERATURE REVIEW

A lot of research work has been carried out for predicting the cutting forces in drilling. A brief review of literature is being presented here.

Armarego and Cheng [1] developed a cutting analysis, based on oblique cutting models, for the drill lips of flat rake face (modified) drills. The analysis predicted reasonable deformation and force distributions along the drill lips. An analysis for conventional drills was also attempted with less success. The concept of geometrical similarity was studied and was found to be useful for prediction of forces in drilling and for the design of twist drills.

Armarego and Cheng [2] predicted effect of geometrical similarity on the deformation and forces of different sized conventional and modified drills experimentally. The flat rake face modified drill considerably reduced the forces in drilling. The cutting analyses for the lips of modified drills were found to be qualitatively and quantitatively sound. Statistical methods were used to process the data and verify the theoretical predictions.

Usui *et al.* [3] proposed a new model of chip forming process in three dimensional cutting with single point tool. The process was interpreted as a piling up of orthogonal cuttings along the cutting edge. Based upon the proposed model, an energy method similar to the upper bound approach, which enabled to predict the chip formation and the three components of cutting force by using only the orthogonal cutting data was developed. The method was also applied to predict chip formation and cutting force in oblique cutting, plain milling, and groove cutting operations. The cutting model and the energy method developed were further extended to predict chip formation and cutting force in machining with conventional single-point tool. The prediction was concluded to be possible in the practical range of cutting conditions regardless of size of cutting and tool geometry. The predicted results were verified to be in good agreement with the experimental results in a wide variety of depth of cut, side and back rake angles, side cutting edge angle, and nose radius.

Carroll *et al.* [4] described two computer models that treated the special case of orthogonal cutting. The models were based on the finite element method, which was used to discretize a portion of the workpiece in the vicinity of the cutting tool. From the models, the detailed stress and strain fields in the chip and workpiece, chip geometry and tool force was determined. The first model was based on a specially modified version of a large deformation updated Lagrangian code, which employed an elastic-plastic material model. The second model treated the region in the vicinity of the cutting tool as an Eulerian flow field. Material passing through the field was modeled as viscoplastic. Results obtained from both models showed excellent agreement when compared with measured tool forces for slow speed cutting of Aluminum 2024-T361.

Rubenstein [5] studied the expression for torque and thrust force generated by spade drills with a view to determine their applicability to twist drill. Accordingly it was concluded that to every twist drill an equivalent spade drill could be found, the condition of equivalence being that the chip deflection and the chip thickness ratio produced by the spade drill are the same as those produced by the twist drill. It followed that expression for the torque and the thrust which was applicable to spade drills were equally applicable to twist drills.

Kug *et al.* [6] developed a cutting model by applying the thermo-viscoplastic Finite Element Method (FEM) to analyze the mechanics of steady state orthogonal cutting process. The model was capable of dealing with free chip geometry and chip-tool contact length. The coupling with thermal effects was also considered. In calculating temperature distributions, the "upwind" scheme was employed to remove spurious oscillations that occur in the solution and therefore it was possible to analyze high speed metal cutting. Orthogonal cutting experiments are performed for 0.2% carbon steel to validate the cutting model. Tool forces were measured and the results discussed in comparison with the results of the FEM analysis.

Chandrasekharan *et al.* [7] developed models to predict the thrust and torque forces at the different regions of cutting on a drill. The mechanistic approach adopted to develop these models exploits the geometry of the process, which was independent of the workpiece material. The models were calibrated to a particular material using the well

established relationship between chip load and cutting forces, modified to take advantage of the characteristics of the drill point geometry. The cutting lips model predictions agreed well with the experimental data for both materials, chisel-edge model proposed for metals agreed well with the experimental data.

Chandrasekharan *et al.* [8] developed a model to predict the forces for arbitrary drill point geometry. The cutting-lips were divided into the elements and the elemental forces were determined from a fundamental oblique cutting model. The method was developed to parametrically define the cutting-lip in three dimensional space and to determine the oblique cutting parameters (cutting angles and chip thickness) at each element on the cutting lip. The model did not require calibration experiments for each point geometry. Here the conical drill was used to determine the model co-efficient for a tool and work-piece material combination and these were used for the other drill point geometry.

Bergstrom *et al.* [9] developed a model for predicting torque and thrust in drilling using a minimum cutting energy method for predicting the chip flow angle. The model has been experimentally verified and the minimum cutting energy model was shown to predict thrust and torque more accurately than the more commonly used Stabler's Rule.

Min *et al.* [10] introduced a finite element model of the burr formation of two-dimensional orthogonal cutting and validated with experimental observations. A detailed and thorough examination of the drilling burr forming process was undertaken. The information was then used in the construction of an analytical model and, leads to development of a three dimensional finite element model of drilling burr formation. Using the model as a template, related burr formation problems that have not been physically examined were simulated and the results used to control process planning resulting in the reduction of burr formation.

Guo *et al.* [11] developed thermo-elastic-viscoplastic explicit FEM model to predict effects of sequential orthogonal cuts on the mechanical state and cutting mechanisms in a machined layer. Residual stress distribution was shown to be significantly changed and cutting mechanisms slightly changed in sequential cuts. A method to compressively pre-stress a sequentially machined surface was proposed by planning the uncut chip

thickness. An evaluation of effects of unloading of cutting forces, cutting temperatures, and clamping forces on the residual stress distribution was done.

Strenkowski *et al.* [12] developed a model of three-dimensional cutting for predicting tool forces and the chip flow angle. The approach consisted of coupling an orthogonal finite element cutting model with an analytical model of three-dimensional cutting. The finite element model was based on an Eulerian approach. The analytical model developed by Usui *et al.* [3]. was used, in which a minimum energy approach was used to determine the chip flow direction. The model developed by Usui *et al.* [3] required orthogonal cutting test data to determine the tool forces and chip flow angle. A finite element model was used to supply the orthogonal cutting data for model from Usui *et al.* [3]. With this approach, a predictive model of three-dimensional cutting was developed that does not require measured data as input. Cutting experiments described were in good agreement between measured and predicted tool forces and chip flow angles for machining of AISI 1020 steel.

Strenkowski *et al.* [13] developed an analytical finite element technique for predicting the thrust force and torque in drilling with twist drills. The approach was based on representing the cutting forces along the cutting lips as a series of oblique sections. Similarly, cutting in the chisel region was treated as orthogonal cutting with different cutting speeds depending on the radial location. For each section, an Eulerian finite element model was used to simulate the cutting forces. The section forces were combined to determine the overall thrust force and drilling torque. Good agreement between the predicted and measured forces and torques was found in orthogonal and oblique cutting and in drilling tests. The drilling tests were performed on AISI 1020 for several drill diameters, spindle speeds, and feed rates.

Pirtini *et al.* [14] developed a new mathematical model based on the mechanics and dynamics of the drilling process for the prediction of cutting forces and hole quality. A new method was also proposed in order to obtain cutting coefficients directly from a set of relatively simple calibration tests. The model was able to simulate the cutting forces for various cutting conditions in the process planning stage. In the structural dynamics module, measured frequency response functions of the spindle and tool system was

integrated into the model in order to obtain drilled hole profiles. Therefore, in addition to predicting the forces, the new model allows the determination and visualization of drilled hole profiles in 3D and to select parameters properly under the manufacturing and tolerance constraints.

Bakkal *et al.* [15] investigated the thrust force, torque, and tool wear in drilling of Zr-based Bulk Metallic Glass (BMG) material. Drilling the BMG at high speed generated the chip light emission, high tool temperature, and severe tool wear. At low spindle speed, the BMG work-material builds up at the major and margin cutting edges and may break the drill. A range of feasible spindle speed and feed rate for the efficient drilling of BMG without the detrimental chip light emission and cutting edge work-material build-up has been identified in this study. Under the same drilling condition, the WC-Co tool generally required less thrust force and about the same torque than the high-speed steel tool. The progressive wear of the major and margin cutting edges for BMG drilling was examined. Severe drill wear was associated with the bright BMG chip light emission. Without chip light emission, the drill wear was visible but not severe.

Ming-Hung Hsu [16] predicted the dynamic characteristics of the drilling process. A pre-twisted Bernoulli-Euler beam was used to simulate the drill. The Eigen value problem of a rotating pre-twisted beam under axial loading on an elastic foundation was numerically formulated using the Differential Quadrature Method (DQM). Effects of the number of sampling points, rotation speed, pre-twist angle, axial loading, and elastic foundation stiffness on the calculated natural frequencies were also studied. Numerical results demonstrate the validity and the efficiency of the DQM in treating this type of problem. The computation times using DQM were smaller than the computation times using FEM. A varying-length elastic foundation was used to approximate the drilling process.

Claudin *et al.* [17] determined the suitable cutting tools for the machining of a large welded frame in low carbon steel. Various drill technologies were used in the drilling process such as solid carbide drills, solid carbide modular drills, which consist of coated carbide edges and a sintered steel body or indexable drills. The effects of the drill technologies and the lubricant conditions were compared with taking into account of the

cutting conditions and forces. The objective was to link the cutting forces and it distribution along the cutting edges to the cutting parameters the drill geometry and the cooling conditions.

Dargnat *et al.* [18] proposed a semi-analytical model that allowed the determination of forces on the tool, as well as heat fluxes and temperatures along the edges of the drill. The main cutting edge and the chisel edge were considered. It also took into account the elastic relaxation on the clearance face with edge acuity, as well as a proper modeling of the phenomena occurring at chisel edge in relation with its geometry and the kinetics of a drilling operation.

Nayebi *et al.* [19] developed an analytical model which predicts thrust force in the drilling with a twist drill. The thermomechanical properties were accounted for to describe the material flow in the primary shear zone and at the element–chip interface. The chip flow was determined by the assumption that the friction force on the tool face was collinear to the chip flow direction. The model permitted to predict the chip flow direction, the contact length between the chip and the tool and the temperature distribution at the tool–chip interface which had an important effect on the tool wear. A temperature friction law was introduced and the pressure on the tool–chip interface was modeled. Using the thermo-viscoplastic model and the temperature friction law, the tangential forces, friction coefficient and contact length on the cutting element as a function of radius, for different feed rate and cutting speed, were obtained. The proposed model results were compared with experimental results and good agreement was obtained.

Kwong *et al.* [20] presented a comprehensive analysis and discussions of the influence of the drill's minor cutting edge to workpiece surface integrity and residual stress distribution for RR1000, a newly developed nickel-based super alloy. The effects were critical to the acceptance of the new material in relation to tool geometry and machining strategies. The thickness of material drag in the hoop direction has been found to be the highest at the top and the least at the bottom of the hole, which was directly related to the contact duration between the minor cutting edge and workpiece surfaces; moreover this difference increased at higher levels of wear of the minor cutting edge. On-line process

monitoring techniques have been employed to further understand the material drag phenomena, including feed force, torque and acoustic emission. Compressive axial and tensile hoop stresses at the surface of the holes have been measured as a function of depth and correlated both with metallurgical analysis of drilled surfaces and the process monitoring signals.

As can be seen from the literature review, the researchers developed a number of methods for predicting the forces on the drill. FEM models were also developed for the purpose. In the present work the FEM model developed by Strenkowski *et al.* [12, 13] is used to develop a program in C so that the user can use it for different angles and material. The program was validated using experimental data.

CHAPTER 3 FEM FORMULATION

This chapter gives the details of the FEM model developed by Strenkowski *et al.* [12, 13] which is used for the development of the program.

3.1 SINGLE-EDGE CUTTING MODEL

The model is based on an energy approach in which three-dimensional cutting is approximated as a series of orthogonal slices. Using orthogonal cutting data under equivalent cutting conditions, the chip flow angle and three-dimensional tool forces are determined for single-point tools with a nose radius.

Consider first the simplest case of a tool with a zero nose radius as shown in Fig. 3.1. The inclination angle of the main cutting edge is *i*, the depth of cut is t_1, and the cutting width is *b*. When *i*=0, the cutting configuration is orthogonal. The underlying assumption of the model is that a chip is produced by shear forces acting simultaneously in two planes. The main cutting edge *CD* produces shear in the trapezoidal plane *CEFD*, while the secondary cutting edge *CB* produces shear in the triangular plane *CEB*.

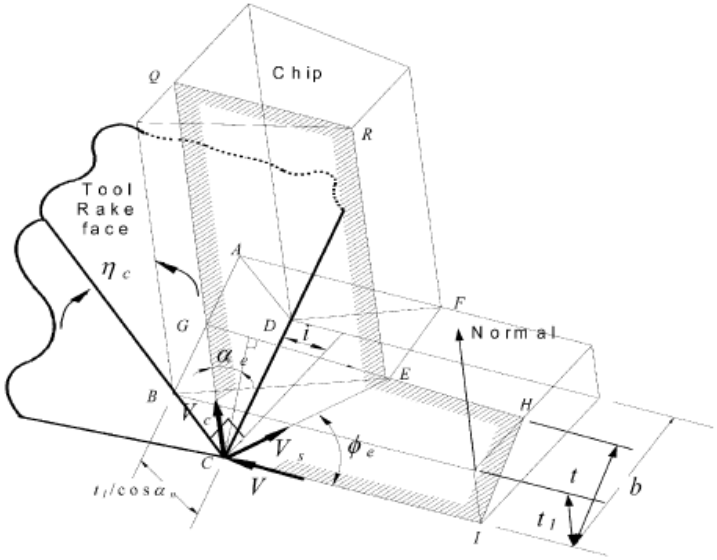

Fig. 3.1 Basic model of double edge cutting, in which the plane IHERQGC represents an orthogonal cutting plane to approximate three-dimensional cutting.

In this approach, three-dimensional cutting is simplified as a collection of plane strain orthogonal cutting slices. One typical plane is represented by *IHERQGC*, which is shown as cross-hatched in Fig. 3.1. This plane is defined by the cutting velocity (*V*) and the chip flow velocity vector (V_C). Chip formation in this plane may be regarded as plane strain deformation with a corresponding shear angle, mean friction angle, and work material shear strength as in orthogonal cutting. Therefore, the line *CE* may be regarded as the shear plane and line *HI* may be considered the undeformed chip thickness in orthogonal cutting. Any other plane that is parallel to the plane *IHERQGC* will have the same effective angle and effective rake angle, but it will have a different depth of cut (*t*). Therefore, three-dimensional cutting is interpreted as a series of orthogonal slices, each with the same effective shear angle and effective rake angle along the main cutting edge.

The effective rake angle (α_e) is measured on the plane which is formed by the chip flow velocity (V_C) and cutting velocity (*V*), and defined by the angle between the chip flow direction and a line normal to the cutting velocity. This angle can be related to the chip flow angle (η_C), the inclination angle (*i*), and the rake angle (α_n) by [3]

$$\alpha_e = \sin^{-1}\left(\alpha_n \cos i \cos \eta_C + \sin \eta_C \sin i\right) \tag{3.1}$$

The chip flow angle (η_C) can be determined using an energy approach. The total cutting energy per unit time ($V.F_H$), where F_H is the principal component of cutting force, is equal to the consumption of shear energy on the shear plane and friction energy on the tool face. The cutting energy is converted into energy on the shear plane and energy due to friction along the rake face. The energy on the shear plane can be written as:

$$U_S = \tau_S V_S A \tag{3.2}$$

Where *A* is the total shear plane area, and V_S and τ_S are the velocity and shear stress on the shear plane, respectively. The area *A* consists of the triangle *CEB* (A_1), and the trapezoid *CEFD* (A_2) shown in Fig. 3.1. It is shown that the area can be written as explicit functions of the shear angle, inclination angle, effective rake angle, normal rake angle, and chip flow angle. Also from orthogonal theory, the velocity in the shear plane is given by:

$$V_S = \frac{\cos\alpha_e}{\cos(\phi_e - \alpha_e)} V \tag{3.3}$$

Where ϕ_e is the angle between the shear velocity and cutting velocity, α_e is the effective rake angle. Thus, the shear energy rate (U_S) in Eq. (3.2) may be rewritten as:

$$U_S = \frac{\tau_S (A_1 + A_2)\cos\alpha_e}{\cos(\phi_e - \alpha_e)} V \tag{3.4}$$

The friction energy rate (U_f) on the rake face is found by a similar analysis [3] as:

$$U_f = F_t \frac{\sin\alpha_e}{\cos(\phi_e - \alpha_e)} V \tag{3.5}$$

In order to calculate the total energy rate from Eq. (3.4) and (3.5), the effective shear plane angle (ϕ_e) and the shear plane stress (τ_S) must be known. It is assumed that the relationships between ϕ_e and τ_S and the effective rake angle (α_e) are the same as those in orthogonal cutting under equivalent conditions. In addition, by assuming that the friction force acting on the unit width of the tool face with undeformed chip thickness (*t*) is the same as the friction force in orthogonal cutting with unit width of cut and undeformed chip thickness (*t*), the friction force (F_t) can be written as [13]:

$$F_t = \frac{\tau_S \sin\beta\cos\alpha_e}{\cos(\phi_e + \beta - \alpha_e)\sin\phi_e} Q \tag{3.6}$$

Where β is the friction angle on the tool face and *Q* is given for a sharp tool to be:

$$Q = \frac{bt_1}{\cos i \cos\alpha_n} \tag{3.7}$$

These equations can be used to evaluate the friction energy rate (U_f) in Eq. (3.5).

The total cutting energy can be found by adding the contributions from the shear and friction energy rates. Note that the energy rates are dependent on the chip flow angle (η_C) which is not known. However, the angle can be found from the condition that the chip will flow in a direction that minimizes the cutting energy (*U*).

The principal tool force (F_H) can be derived from equilibrium of energy to be [3]:

$$F_H = \left\{ \frac{\tau_S \cos\alpha_e}{\cos(\phi_e - \alpha_e)} \left[(A_1 + A_2) + \frac{bt_1 \sin\beta}{\cos(\phi_e + \beta - \alpha_e)\cos i \cos\alpha_n} \right] \right\} \quad (3.8)$$

The normal force (N_t) can be determined from the Eq. (3.9):

$$N_t \cos\alpha_n \cos i + F_t \sin\alpha_e = F_H \quad (3.9)$$

Once N_t is known, the vertical force (F_V) and transverse force (F_T) components can be written in terms of the normal force (N_t):

$$F_V = -N_t \sin\alpha_n + F_t \quad (3.10)$$

$$F_T = -N_t \cos\alpha_n \sin i + F_t \sin\eta_C \cos i - F_t \cos\eta_C \sin i \sin\alpha_n \quad (3.11)$$

Where F_T is the friction force. In orthogonal cutting tests are necessary to provide the shear stress (τ_S), shear angle (ϕ_e), and friction angle (β) needed in the above equations. The force components are functions of α_n, i, b, t_1 and η_C. For any cutting condition, the parameters α_n, i, b, t_1 are known constants, while the chip flow angle (η_C) can be evaluated using the energy method. Therefore, the three-dimensional tool forces are determined.

3.2 DRILLING MODEL

The analytical finite element oblique cutting technique described in the previous section is applied to selected sections along the cutting lip to determine the drilling forces. At each oblique cutting section, the three-dimensional cutting forces are calculated and then combined to determine the drilling thrust force and torque. The geometry of a typical twist drill as defined in terms of three key parameters, the helix angle, point angle (2ρ) and web-thickness ($2w$) have been presented in [21]. Both the helix angle and the point angle will affect the rake angle along each cutting lip. A large helix angle results in a more positive rake angle, which improves the cutting efficiency but also weakens the drill.

3.2.1 Cutting Lip Force Model

For the drilling model, each cutting lip is divided into oblique cutting sections for which the corresponding three-dimensional forces can be determined. For each section, the rake and inclination angle must be determined. For straight cutting lips, the inclination angle (i) and normal rake angle (α_n) can be determined by the following formula [21]:

$$\sin i = \frac{w \sin \rho}{r} \tag{3.12}$$

$$\tan \alpha_n = \cos i \left(\tan \alpha_S \cos C_S + \tan \alpha_b \sin C_S \right) \tag{3.13}$$

Where

$$\tan \alpha_S = \frac{\tan \delta}{\tan C_S} - \frac{\tan i}{\sin C_S} \tag{3.14}$$

$$\cos C_S = \frac{\cos \rho}{\cos i} \tag{3.15}$$

$$\tan \alpha_b = 2\pi \frac{r}{L} \tag{3.16}$$

$$\delta = \tan^{-1}\left(2\pi \frac{r}{L} \right) \tag{3.17}$$

In the above equations, w is the half web thickness, r is the radial distance from the drill axis, and L is the pitch length of the helix on the drill.

Although the normal rake angle is highly negative near the chisel edge, the inclination angle is more positive. These angles compensate for each other so that the effective rake angle remains positive or slightly negative near the chisel edge.

Using the single edge oblique cutting model, forces in the horizontal, vertical, and lateral directions can be determined. Note that forces are based on a local coordinate system for each section along each cutting lip. These local forces must be transformed to the global coordinate system corresponding to the radial, axial, and transverse directions of the drill. Forces in the axial direction contribute to the thrust force. The torque consists of the transverse force times the radial distance to the axis of the drill. The forces in the radial direction cancel each other due to the symmetry of the cutting lips.

Fig. 3.2 shows the directions of the local F_H , F_V and F_T forces and global force components $F_{\tan g}$, F_{thrust}, F_{rad} for a typical radial location along a drill cutting lip. The equations for transforming local oblique cutting forces to the global drill coordinates are:

$$F_{\tan g} = F_H \tag{3.18}$$

$$F_{thrust} = F_T \cos\rho + F_V \frac{\sqrt{\left(r^2 - w^2\right)}}{r} \sin\rho \tag{3.19}$$

$$F_{rad} = F_T \frac{\sqrt{\left(r^2 - w^2\right)}}{r} \sin\rho + F_V \cos\rho \tag{3.20}$$

Note that in general, cutting edges in a drill are curved and not necessarily straight as shown in Fig. 3.2. Only certain combinations of the helix angle, point angle, and radius of flute can produce a straight cutting lip.

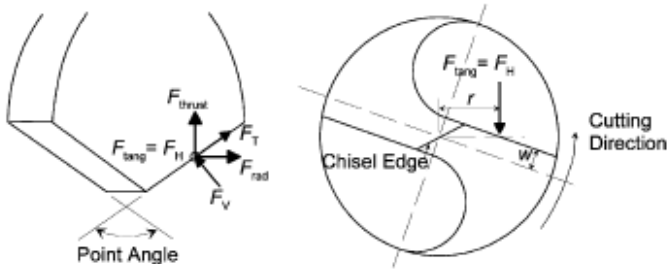

(a) **(b)**

(a)Side view, (b) Top view

Fig. 3.2 Conversion of F_H, F_V, and F_T in oblique cutting to F_{rad}, F_{thrust}, and F_{tang} on a drill.

3.2.2 Chisel Edge Force Model

The majority of the material removed by a drill occurs from the cutting action of the cutting lips. In contrast, the chisel edge provides support during drilling. Cutting along the chisel edge is not efficient due to the large negative rake angle and the slow cutting speed near the center of the drill. The cutting forces along the chisel edge typically contribute more than half of the total thrust force, while only contributing a very small portion of the drilling torque. Although the chisel edge removes little material, it plays an

important role in providing drill point strength to resist lateral bending moments due to vibration or unbalanced forces during drilling.

Cutting within the chisel edge region is treated as equivalent orthogonal cutting slices. The cutting speed for each slice depends on the distance from the centerline. The cutting speed varies from nearly zero at the center of the drill to its maximum at the transition with the cutting lip.

For a typical drill with a 118^0 point angle, the rake angle for an orthogonal section in the web region is 59^0. Cutting under such a negative rake angle is very difficult to model with an updated-Lagrangian finite element formulation. However, an Eulerian approach can be successfully applied for orthogonal cutting with large negative rake angles, as long as the mesh is carefully designed.

CHAPTER 4 RESULTS AND DISCUSSION

The purpose of the present work is to investigate the thrust force in drilling. An analytical finite element technique is used for predicting the thrust forces in drilling using twist drill. A program, developed in C language is used to calculate the values of the various forces acting on the drill using the oblique cutting method.

4.1 FEM MODEL

The FEM formulation is applied to selected section along the cutting lip to determine the drilling force. The FEM drilling model is based on representing the drill point geometry as a series of oblique sections. An analytical model for oblique cutting is first used to analyze a single section in the cutting lip region of the drill. Results of these sections are then combined to determine the thrust force and torque for various operating conditions. The geometry of a typical twist drill, defined in terms of the key parameters, the helix angle, point angle and web thickness as shown in Fig. 4.1.

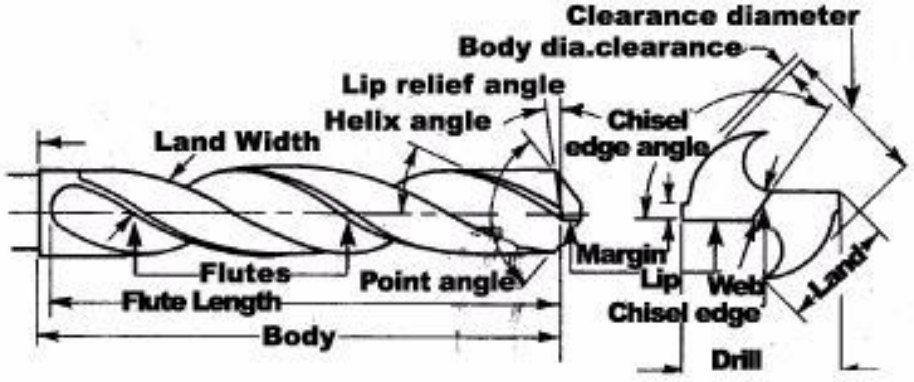

Fig. 4.1 Twist Drill Geometry.

In the finite element model, five sections were used to represent each cutting lip and four sections were used to model the chisel edge. Table 4.1 lists the geometry of each section for a twist drill with a 12.7 mm diameter, 30^0 helix angle, 118^0 point angle drill, 1.70 mm web thickness, and 302 rpm spindle speed. For each section, the table lists the radial location of the section, the cutting speed, depth of cut, width of cut, inclination angle, rake angle, chip flow angle, and effective rake angle. Note that from the outer to the inner drill radius, the effective rake angle decreases and the inclination angle increases for each

section which indicates that the cutting action is becoming more oblique. Throughout the chisel edge region, orthogonal conditions are in effect so that the inclination angle is zero and the rake angle has a large negative value. For drilling of AISI 1020 steel, the forces for each section are also shown in this table. As expected, the radial force (F_{rad}) is zero in the chisel edge region.

Table 4.1 Sections of oblique cutting for drilling with 12.7 mm diameter, 30^0 helix angle, 118^0 point angle, 1.70 mm web thickness, and 302 rpm spindle speed.

r	Cutting speed V	Depth of cut t_1	Width of cut b	Inclination angle i	Rake angle α_n	Chip flow angle η_c	Effective Rake angle α_e	F_{tang}	F_{rad}	F_{thrust}	Torque, $F_{tang}.r$
(mm)	(mm/s)	(mm)	(mm)	(^{0})	(^{0})	(^{0})	(^{0})	(N)	(N)	(N)	(N.mm)
5.82	183.9	0.051	1.04	7.7	28.3	1	28.2	95.1	30.2	39.6	554
4.78	151.1	0.051	1.04	8.8	22.3	4	22.9	100	32.9	40.4	476
3.73	118.1	0.051	1.04	11.3	15.1	6	16.0	107	36.1	43.9	398
2.69	85.1	0.051	1.04	15.7	6.0	11	8.7	118	42	49.3	318
1.63	51.3	0.051	1.04	26.6	-8.6	21	2.0	143	57.3	57	233
0.97	30.5	0.051	0.28	0	-59.0	0	-59.0	35.9	0	64.5	34.8
0.69	21.6	0.051	0.28	0	-59.0	0	-59.0	35.9	0	64.5	24.8
0.41	13.0	0.051	0.28	0	-59.0	0	-59.0	35.9	0	64.5	14.7
0.14	4.3	0.051	0.28	0	-59.0	0	-59.0	35.9	0	64.5	5.03

4.2 RESULTS AND VALIDATION

A program is developed to calculate the various parameters used to determine the various forces acting on the drill bit. All the variables were taken of the type "double" in order to gain maximum accuracy possible. A wide range of predefined mathematical functions are used for calculation purpose. Firstly the mesh was generated with quadrilateral elements. The relationships between ϕ_e, τ_S, β and the effective rake angle (α_e) is adapted from the FEM model developed by Strenkowski *et al.*[12].The shear stress (τ_S) varied linearly from 568 *MPa* for a zero rake angle to 548 *MPa* for a 20° rake for AISI 1020 steel. Fig. 4.2 shows the friction and shear plane angles for several rake angles. The friction angle (β) is found from the vertical and principal force components, which are also computed with the finite element model. Finally, the shear plane angle (ϕ_e) is derived from the chip geometry as the slope of a line between a maximum nodal strain rate and a node on the cutting edge of the tool. Note that the shape and thickness of the chip is iteratively determined with the finite element model.

The advantage of using the finite element model instead of orthogonal cutting experiments is that data can be obtained more readily than from cutting tests. In addition, tool shapes other than flat tools with sharp edges can be simulated. For example, the finite element model allows for the introduction of a radius on the cutting edge. Other tool shapes can also be simulated, such as groove and obstruction type tools.

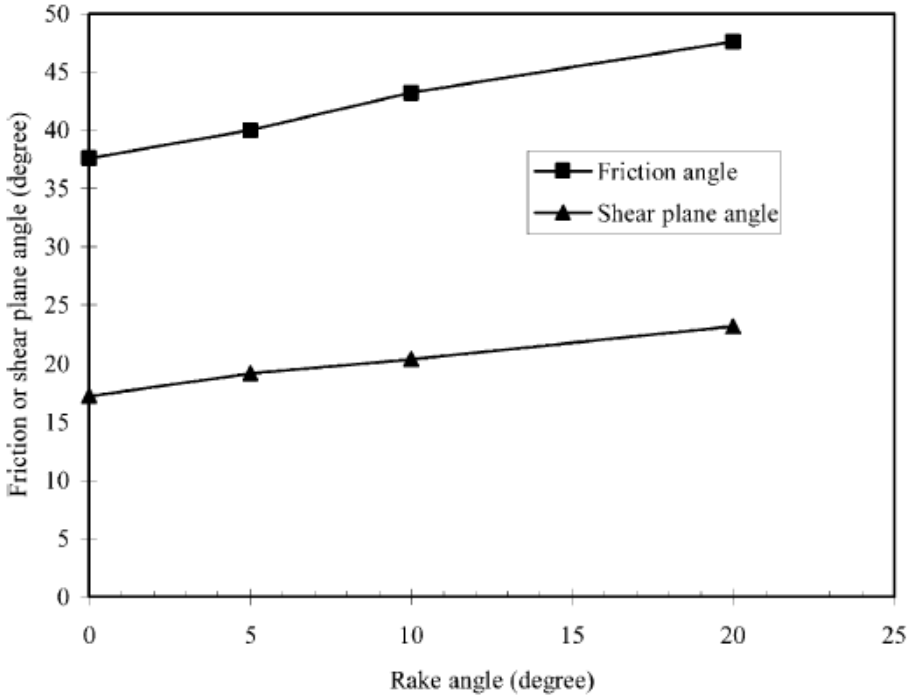

Fig. 4.2 Predicted orthogonal friction and shear plane angles for AISI 1020.

The calculated Principal force (F_H), Vertical force (F_V) and Transverse force (F_T) using the above parameters for the five inclination angles are as shown in Fig. 4.3. The negative value of F_T merely depicts that the direction of the force applied. It is opposite to the direction assumed and is hence ignored while plotting the chart.

The local oblique cutting forces are transformed into global Drill co-ordinates. The values of Tangential force ($F_{\tan g}$), Thrust force (F_{thrust}) and Radial force (F_{rad}) for the five inclination angles are calculated using the local forces F_H, F_V and F_T. The global forces calculated are as shown in Fig. 4.4.

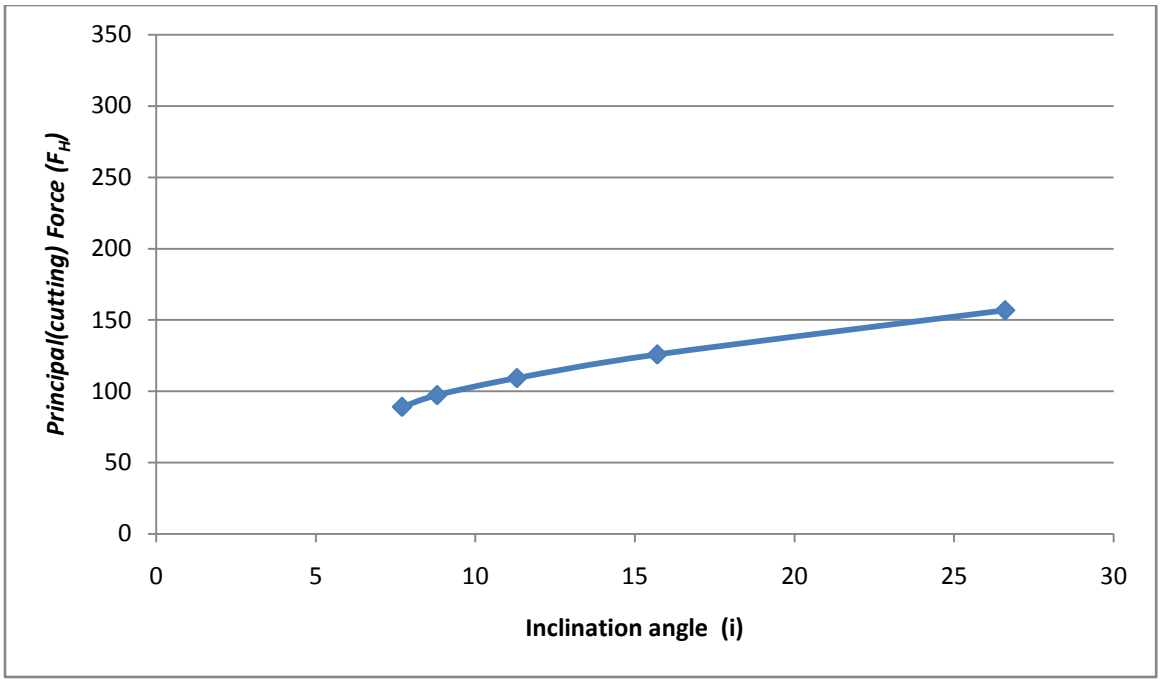

(a) Principal(cutting) Force(F_H)

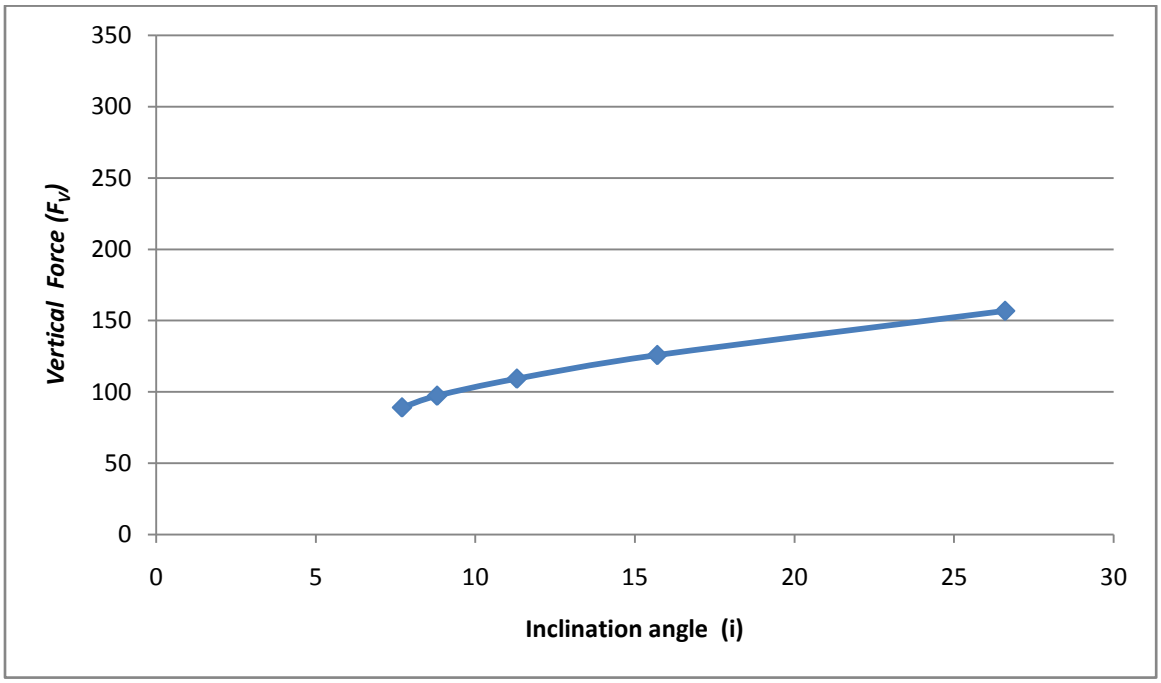

(b) Vertical Force (F_V)

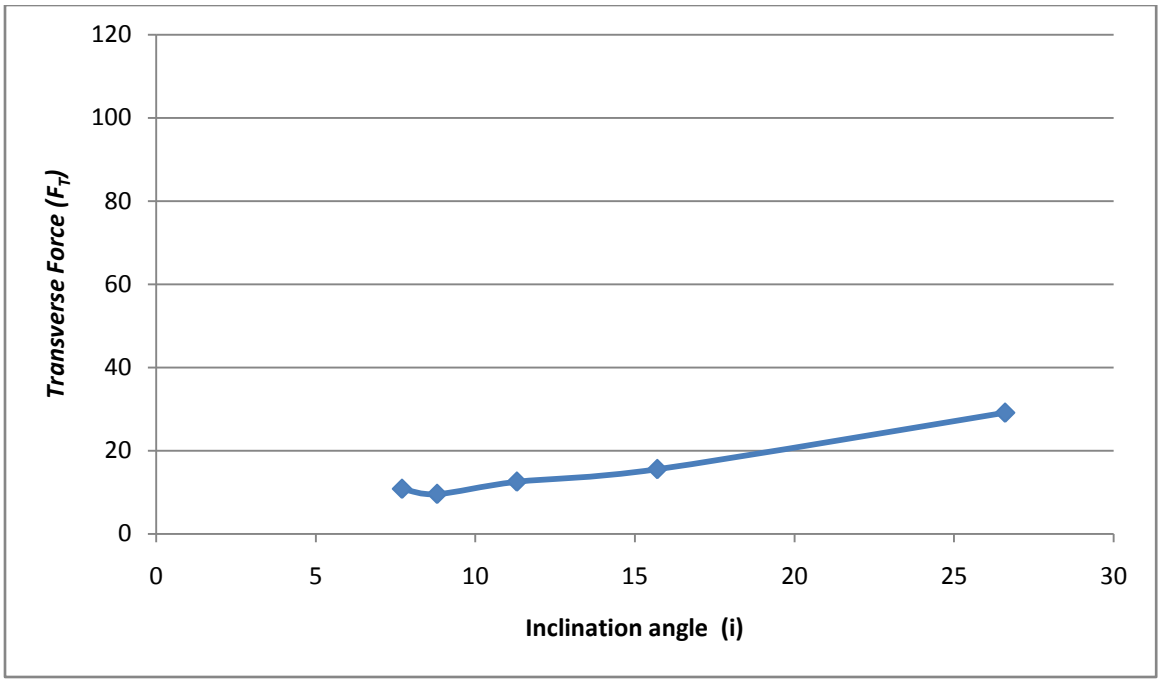

(c) Transverse Force (F_T)

Fig. 4.3 Variation of various primary forces for the five inclination angles.

As seen from the figure the Principal (cutting) force (F_H) and the Vertical force (F_V) rise steeply upto $i = 10^0$ beyond which it attains a nearly straight line pattern.

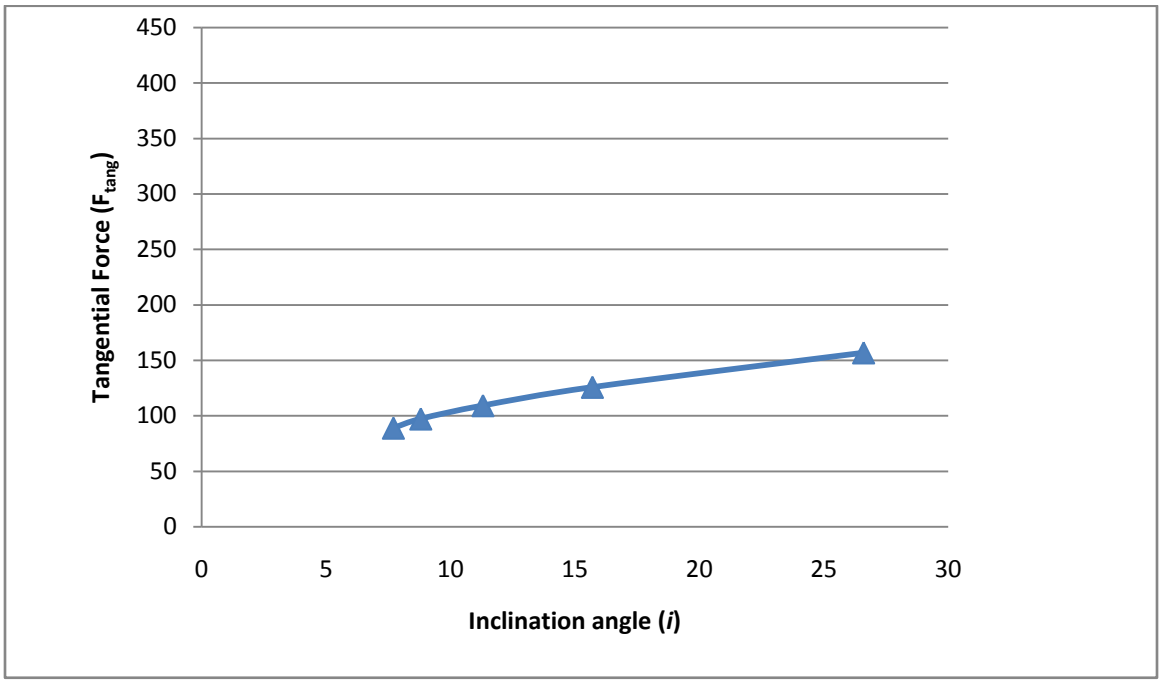

(a) Tangential Force

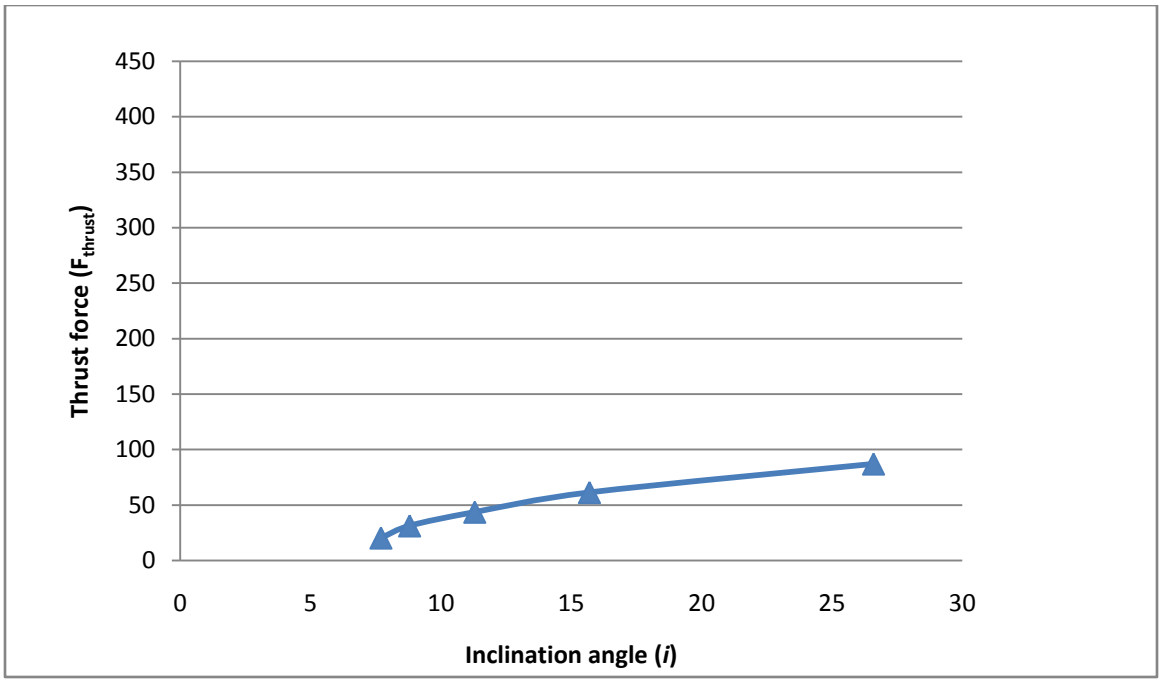

(b) Thrust Force

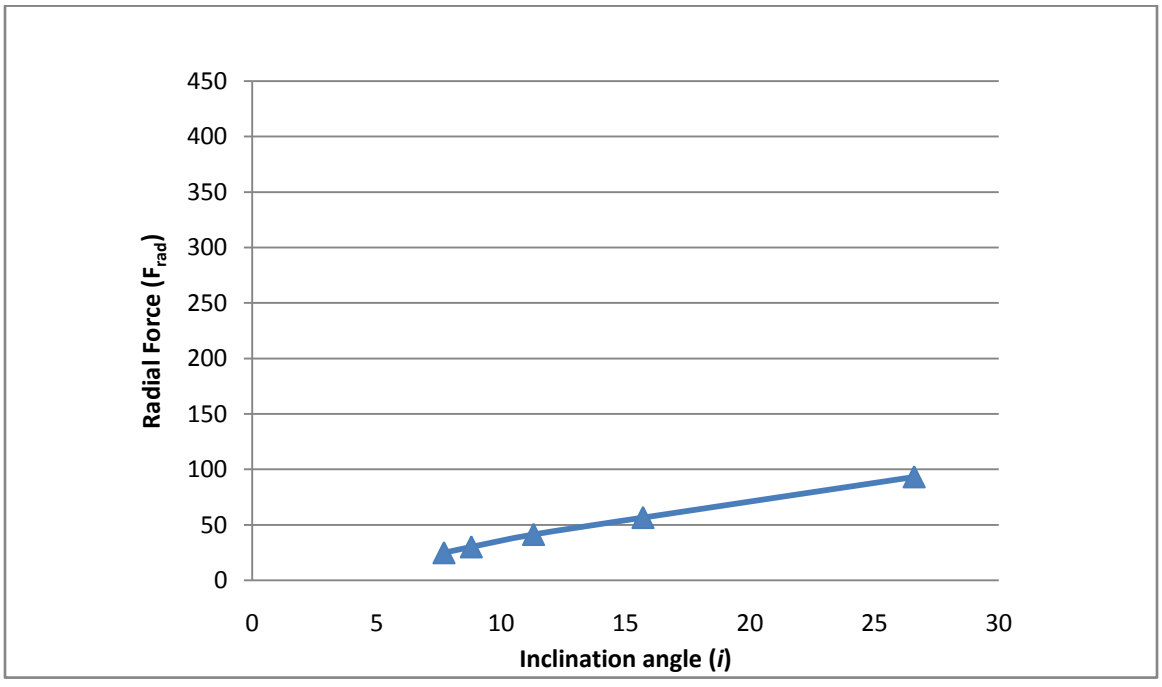

(c) Radial Force

Fig. 4.4 Variation of various global forces for the five inclination angles.

The global forces Tangential force ($F_{\tan g}$), Thrust force (F_{thrust}) and Radial force (F_{rad}) also exhibit a similar trend as shown by the local forces *i.e.* they show a steep rise in the value of the forces in the range of $i = 8^0 - 12^0$.Beyond this range the values keep rising but with a very gradual slope. The Tangential force ($F_{\tan g}$) is the highest among the three forces as it is the actual force acting along the lip of the drill .The values of the forces from the program were needed to be verified in order to ensure the validity of the output obtained.

Thereafter, a comparison of the experimental and calculated forces was made. The experimental results from Strenkowski *et al.* [13] are taken for validation of the program. A comparison of the experimental and calculated forces with respect to inclination angle and effective rake angle is shown in Fig. 4.5 and Fig. 4.6 respectively.

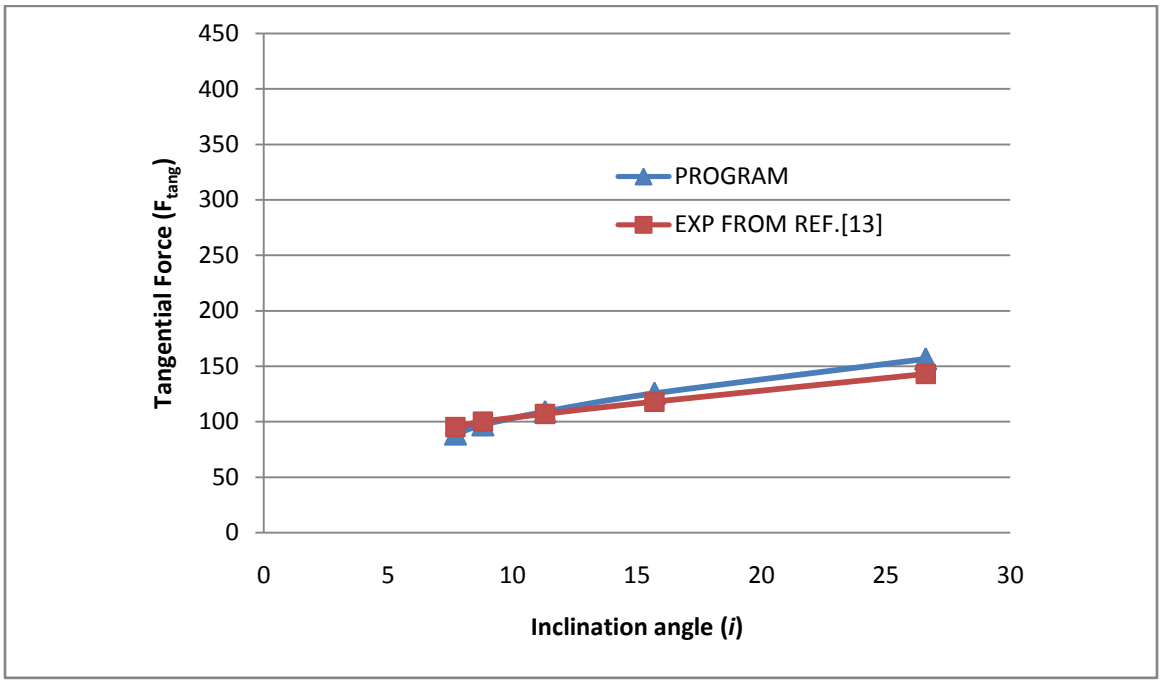

(a) Tangential Force (F_{tang})

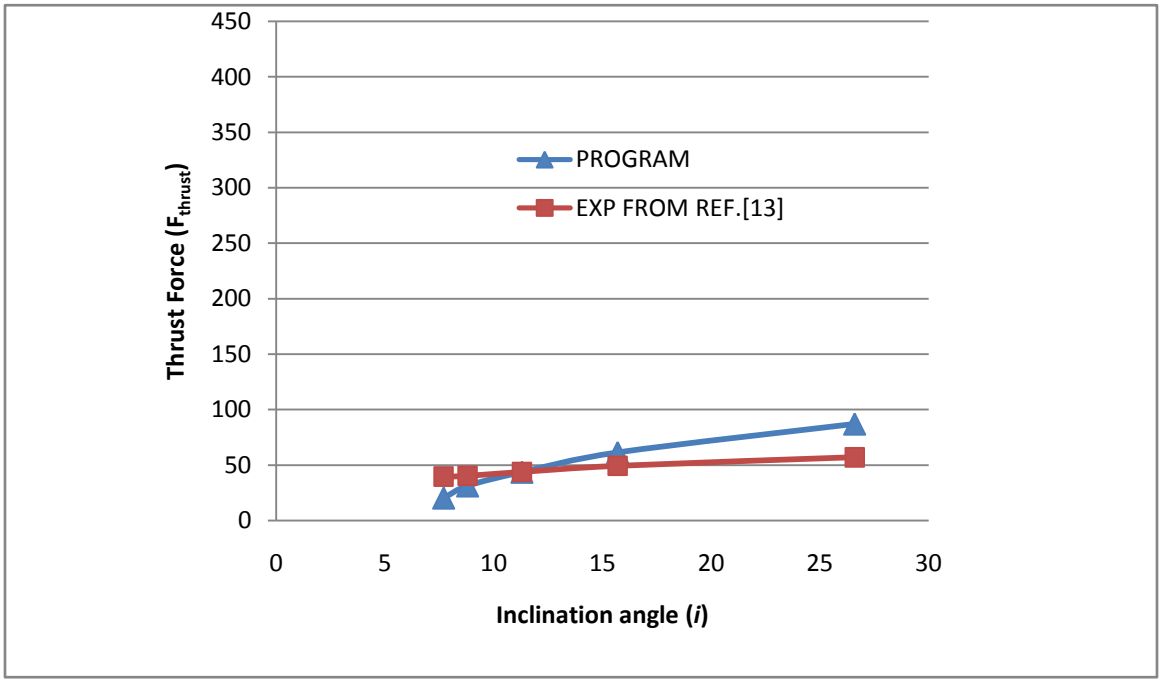

(b) Thrust Force (F_{thrust})

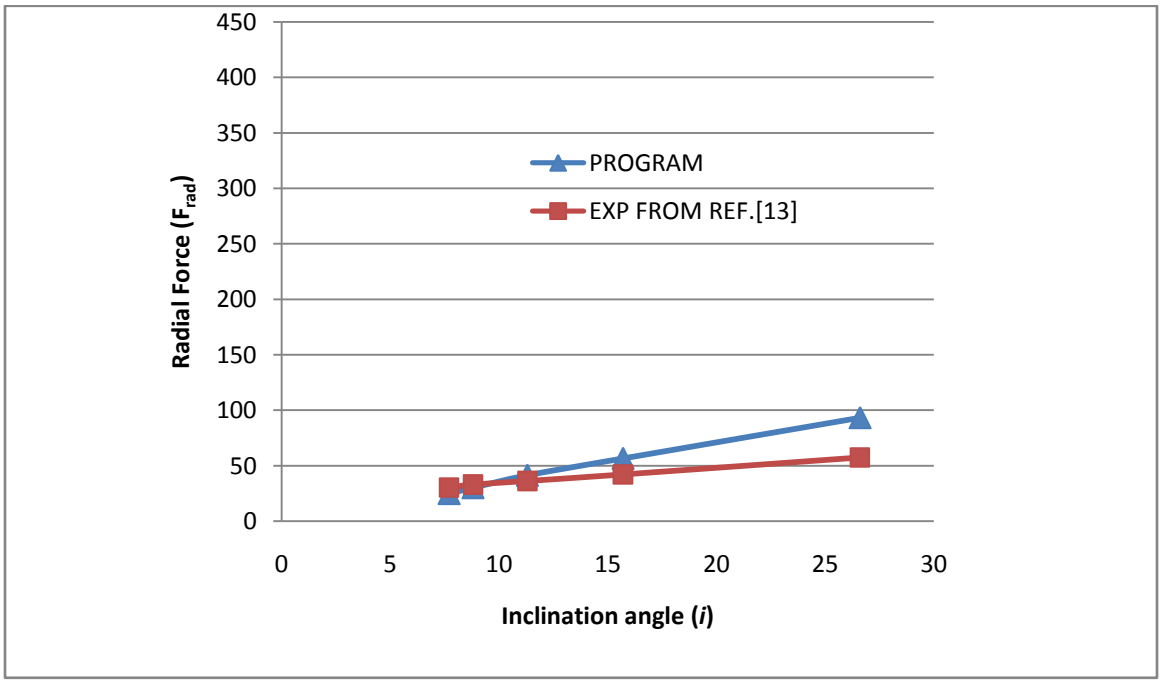

(c) Radial Force (F_{rad})

Fig. 4.5 Comparison of the calculated and experimental values of the global forces for the five inclination angles.

The values with respect to Effective Rake angle (α_e) are as follows.

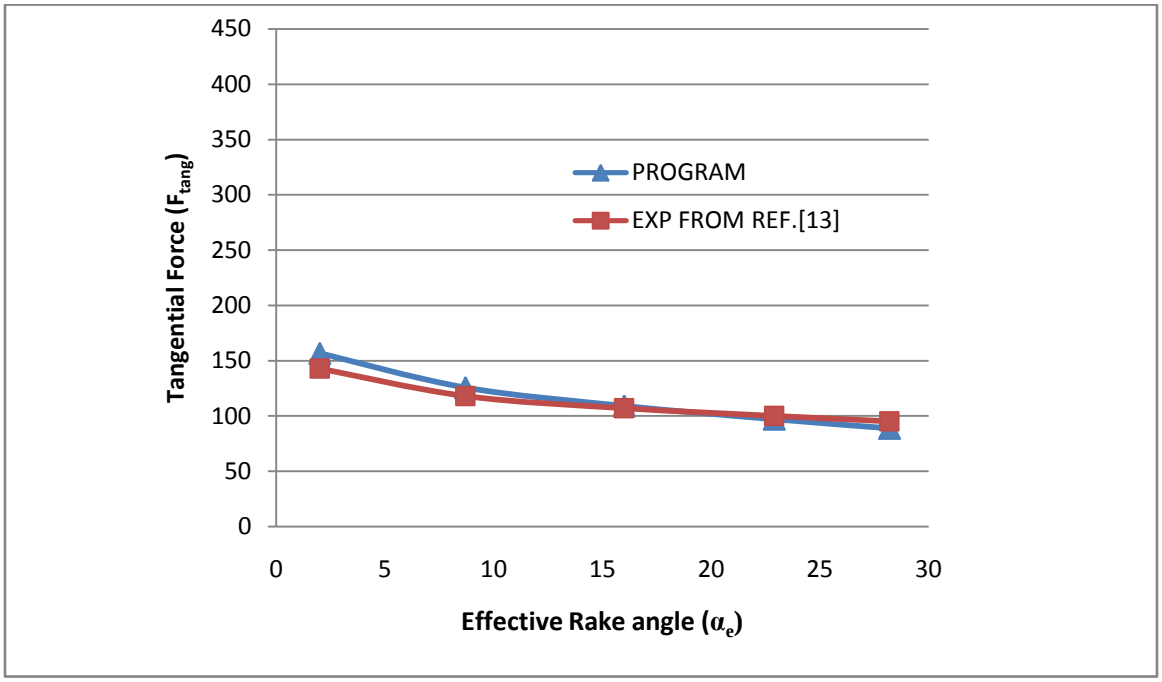

(a) Tangential Force (F_{tang})

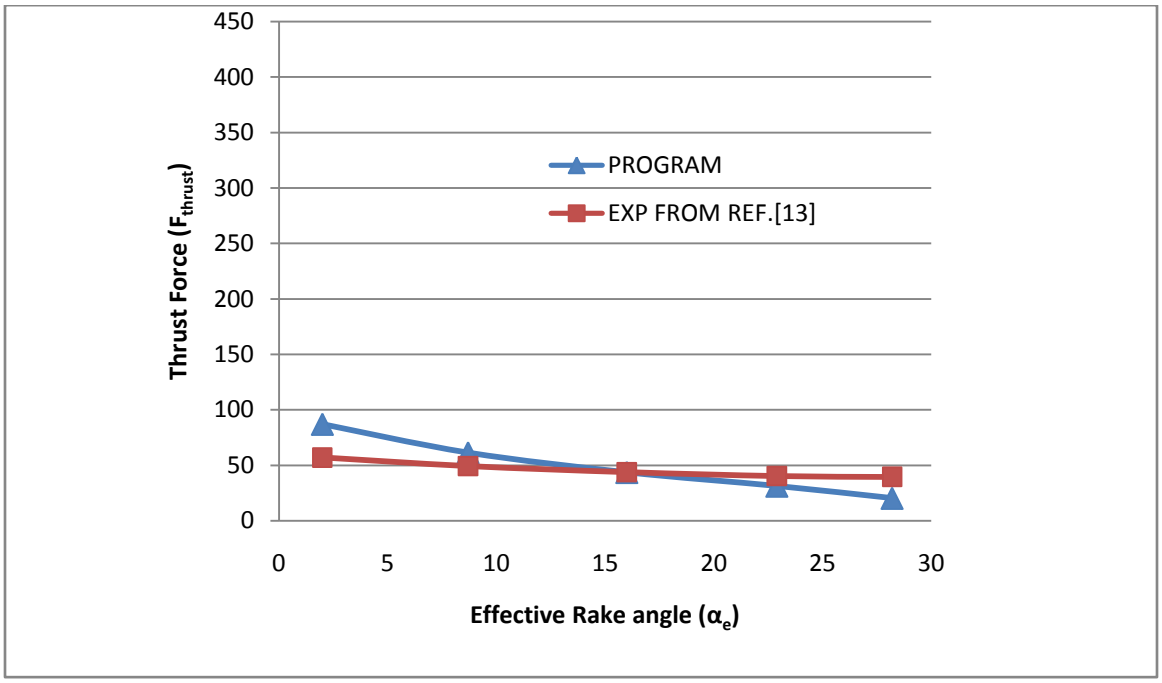

(b) Thrust Force (F_{thrust})

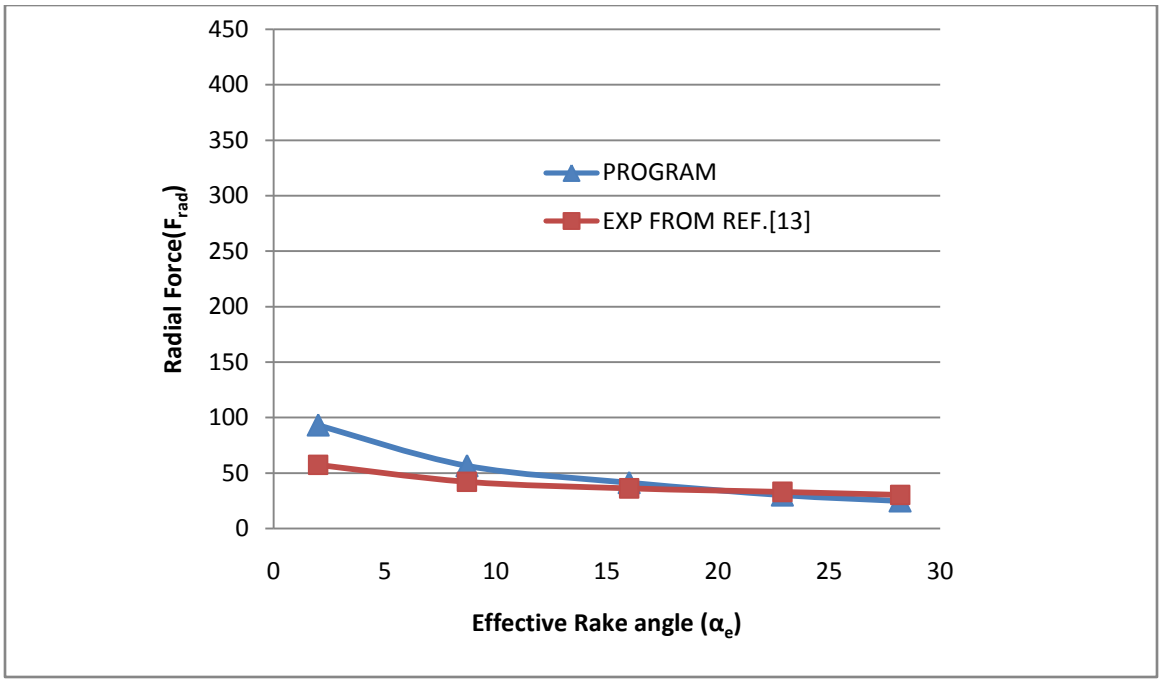

(c) Radial Force

Fig. 4.6 Comparison of the calculated and experimental values of the global forces for the various effective rake angles.

The values of the forces obtained from the program and the reference show a good agreement. For the values of $i = 8^0 - 12^0$ the values show a very high level of accuracy. Due to the limitation of the model available the values beyond the given range showed slight variation. In general, cutting edges in a drill are curved and not necessarily straight as shown in Fig. 3.2. Only certain combination of helix angle, point angle and radius of flute can produce a straight cutting lip [13]. Hence there is a significant variation between the calculated and the experimental values and the values coincide at an inclination angle of $8^0 - 12^0$. The negative value of F_{rad} merely depicts that the direction of the force applied *i.e.* it is opposite to the direction assumed and is hence ignored while plotting the chart.

A good agreement between the measured and experimental values validates the program using the FEM model.

CHAPTER 5 CONCLUSION

5.1 CONCLUSION

An analytical finite element technique developed by Strenkowski *et al.* [12, 13] for predicting the thrust force in drilling with twist drills is used to develop a program in C language. The approach is based on representing the cutting forces along the cutting lips as a series of oblique sections. Similarly, cutting in the chisel region is treated as orthogonal cutting with different cutting speeds depending upon radial location. For each section, a finite element model is used and combined to determine the various forces acting on the drill bit. The results were then validated with the experimental data of Strenkowski *et al.* [13]. Good agreement between both the results was found.

The program is applicable to general drill geometries, under different work piece materials and cutting conditions. It can be readily applied to non-conventional drills other than standard twist drills as the formulation is independent of any specific drill geometry. The advantage of using Eulerian finite element model is that three-dimensional tool forces can be predicted without the need for corresponding cutting (calibration) tests. Therefore design time and development costs will be reduced for new and more complex tool geometries.

5.2 FUTURE SCOPE

The technique can be applied to predict the drill tip temperature, which is an important indicator of drill life. Heat flux from each oblique and orthogonal section can be determined and then be used to calculate the temperature distribution throughout the drill.

REFERENCES

[1] Armarego E.J.A., Cheng C.Y. “Drilling with flat rake face and conventional twist drills - I. Theoretical investigation”, International Journal of Machine Tools and Manufacture, vol. 12, pp. 17-35 (1972).

[2] Armarego E.J.A., Cheng C.Y. “Drilling with flat rake face and conventional twist drills - II. Experimental investigation”, International Journal of Machine Tools and Manufacture, vol. 12, pp. 37-54 (1972).

[3] Usui E., Hirota A., Masuko M., "Analytical prediction of three dimensional cutting process: Part 1 basic cutting model and energy approach, ASME Journal of Engineering for Industry" vol. 100, pp. 222–228 (1978).

[4] Carroll J.T., Strenkowski J.S., "Finite element models of orthogonal cutting with applications to single point diamond turning", International Journal of Mechanical Science, vol. 30, pp. 899–920(1988).

[5] Rubenstein C., “The torque and thrust force in twist drilling—I Theory”, International Journal of Machine Tools and Manufacture, vol.31 pp. 481–489(1991).

[6] Kim Kug Weon, Sin Hyo-Chol, "Development of a thermo-viscoplastic cutting model using finite element method", International Journal of Machine Tools and Manufacture, vol. 36, pp. 379-397(1996).

[7] Chandrasekharan V., Kapoor S.G., DeVor R.E.," A mechanistic approach to predicting the cutting forces in drilling: with application to fiber-reinforced composite materials", Journal of Manufacturing Science and Engineering, vol. 117, pp. 559–570(1995).

[8] Chandrasekharan V., Kapoor S.G., DeVor R.E.," A mechanistic model to predict the cutting force system for arbitrary drill point geometry", S.M. Wu Symposium, vol. 2, pp. 108–114(1996).

[9] Bergstrom Amy J., Filipovic Aleksander J., Olson Walter W., Southerland John W., "Mechanistic prediction of drilling forces incorporating a minimum cutting energy model for chip flow angle", Transactions of NAMRI/SME, vol. 28,pp. 143-148(2000).

[10] Min Sangkee, Dornfeld David A. , Kim Jinsoo , Shyu Borlin “Finite element modeling of burr formation in metal cutting”, Machining Science and Technology, vol. 5, pp. 307-322 (2001).

[11] Guo Y.B., Liu C.R."Fem analysis of mechanical state on sequentially machined surfaces", Machining Science and Technology, vol. 6, pp. 21-41(2002).

[12] Strenkowski J.S., Lin J.C., Shih A.J. “An analytical finite element model for predicting three-dimensional tool forces and chip flow”, International Journal of Machine Tools & Manufacture, vol. 42, pp. 723–731(2002).

[13] Strenkowski J.S., Hsieh C.C. , Shih A.J. “An analytical finite element technique for predicting thrust force and torque in drilling”, International Journal of Machine Tools & Manufacture, vol. 44 pp.1413-1421 (2004).

[14] Pirtini M., Lazoglu I. “Forces and hole quality in drilling”, International Journal of Machine Tools & Manufacture, vol. 45 pp. 1271-1281 (2005).

[15] Bakkal Mustafa, Shihb Albert J., McSpadden Samuel B., Scattergood Ronald O. “Thrust force, torque, and tool wear in drilling the bulk metallic glass”, International Journal of Machine Tools & Manufacture, vol. 45 pp. 863-872 (2005).

[16] Hsu Ming-Hung, “Vibration Analysis of a Drill in the Drilling Process”, International Journal for Computational Methods in Engineering Science and Mechanics, vol. 6, pp. 261-270 (2005).

[17] Claudin, C., Poulachon, G., Lambertin, M. “Correlation between drill geometry and mechanical forces in mql conditions”, Machining Science and Technology, vol. 12, pp. 133-144(2008).

[18] Dargnat, F., Darnis Ph., Cahuc, O. “Energetical approach for semi-analytical drilling modeling”, Machining Science and Technology, vol. 12, pp. 295 -324 (2008).

[19] Nayebi A., Mauvoisinb G., Vaghefpourc H. “Modeling of twist drills wear by a temperature-dependent friction law”, Journal of materials processing technology, vol. 207, pp. 98-106 (2008).

[20] Kwong J., Axinte D.A., Withers P.J., Hardy M.C. "Minor cutting edge–workpiece interactions in drilling of an advanced nickel-based superalloy", International Journal of Machine Tools & Manufacture, vol. 49 pp. 645-658 (2009).

[21] Shaw M.C., "Metal Cutting Principles", Oxford University Press, London (1984).

[22] Ghosh Amitabha, Mallik Ashok Kumar, **"**Manufacturing Science", Affiliated East-West Press (P) Ltd., New Delhi (2009).